ERROR PERFORMANCE OF PHASE SHIFT KEYING SIGNALS IN NONLINEAR CHANNELS

（非線形通信路におけるディジタル位相
変調波の誤り率特性に関する研究　）

IKUO OKA

JANUARY, 1983

ACKNOWLEDGEMENTS

This work has been carried out during a doctoral course under the guidance of Professor Toshihiko Namekawa at the department of Communication Engineering, Faculty of Engineering, Osaka University, Japan.

The author would like to express his appreciation to Professor Toshihiko Namekawa for his guidance, continuing encouragement, and valuable discussion through out this research.

The author would also like to thank Professor Yoshikazu Tezuka, Professor Nobuaki Kumagai, and Professor Yoshiroh Nakanishi, for their creative instruction and guidance.

The author is much indebted to Assistant Professor Norihiko Morinaga for his helpful discussion and untiring efforts in guidance during the preparation of this dissertation.

The author is grateful to Associate Professor Masao Kasahara, Assistant Professor Masashi Murata, and Assistant Professor Masashi Sato for their kind advice and encouragement.

The author is indebted to Professor Hans Marko of Technische Universitaet Muenchen in West Germany for his encouragement, and Dr.-Ing. Guenter Soeder of Technische Universitaet Muenchen for his earniest discussion.

The author wishes to thank Dr. Satoshi Kabasawa of Matsushita Electric Company, Assistant Professor Sung Joon Cho of Han-Kuk Aviation Colledge in Korea, and Dr. Kanshiroh Kashiki of Kokusai Denshin Denwa Co.,Ltd., for their helpful discussion in the early phase of this research. Aknowledgements are also due to Mr. Masato Hata, Dr. Mazen Dahabreh, and all members of Namekawa Laboratory for their earniest discussion on this work.

PREFACE

This thesis investigates the error performance of phase shift keying signals in nonlinear channels where disturbances of both the radio frequency interference and the narrow band Gaussian noise are included. It consists of six chapters which are described as follows.

Chapter 1 provides the background of this thesis, and gives a review of previous and recent researches on the problems which will be discussed in this thesis.

Chapter 2 provides the analytical model of the overall system. As typical nonlinear channels, the satellite channels are introduced, and mathematical representations are expressed for the basic elements used in the model, which are M-ary phase shift keying signals, intersymbol interference, nonlinear channels including radio frequency interference, and detection scheme.

Chapter 3 discusses the error probability of phase shift keying signals in the hard-limiting channel. Considering an intersymbol interference component as the radio frequency interference, the probability density function of the detected phase is derived using the characteristic function method. The error probability is obtained by integrating this probability density function over the error region. A comparison with the linear channel is made to clarify the error probability improvement effects of the hard-limiting channel. Furthermore the effects of cascaded hard-limiters are considered.

Chapter 4 discusses the error probability of phase shift keying signals in the soft-limiting channel. The probability

density function of the detected amplitude is derived with the aid of the Gram-Charlier expansion. Integration of this probability density function over the error region yields the error probability. In order to demonstrate clearly the effects of the soft-limiting channel, a comparison with the linear channel or the hard-limiting channel is also included.

Chapter 5 gives a comparison of the error performance between the phase shift keying signal and the minimum shift keying signal in the hard-limiting channel. For the error probability analysis, an equivalent model is newly proposed. Using this model, the probability density function of the detected amplitude is obtained with the aid of the Gram-Charlier expansion. The error probability is given by integrating this probability density function over the error region. The error performance of the phase shift keying signal and the minimum shift keying signal are compared to show the effects of interference and band-limiting in nonlinear channels. Furthermore the error probabilities of the phase shift keying signal and the minimum shift keying signal in the linear channel are derived to compare with those in nonlinear channels

Chapter 6 summerlizes the overall conclusions obtained in this thesis.

CONTENTS

page

ACKNOWLEDGEMENTS i

PREFACE ii

LIST OF FIGURES vi

CHAPTER

1. INTRODUCTION 1

1.1 Background 1

1.2 Analysis Methods 3

2. SYSTEM DESCRIPTION 7

2.1 Introduction 7

2.2 Phase Shift Keying Signals 7

2.3 Intersymbol Interference 8

2.4 Model for Nonlinear Channels 13

2.5 Detection Scheme 16

2.6 Concluding Remarks 18

3. EFFECTS OF HARD-LIMITING 19

3.1 Introduction 19

3.2 Probability Density Function of Detected Phase 20

3.3 Error Probability 27

3.4 Comparison with Linear Channel 30

3.5 Effects of Cascaded Hard-Limiters 35

3.6 Concluding Remarks 39

4. EFFECTS OF SOFT-LIMITING 40

4.1 Introduction 40

4.2 Probability Density Function of Detected Amplitude. 41

4.3 Error Probability 48

4.4 Concluding Remarks 50

5. COMPARISON WITH MINIMUM SHIFT KEYING SIGNALS 52

5.1 Introduction 52

5.2 Minimum Shift Keying Signals 54

5.3 Equivalent Model for Error Probability Analysis.... 57

5.4 Probability Density Function in Equivalent Model... 59

5.5 Error Probability 68

5.7 Concluding Remarks 74

6. CONCLUSIONS 76

APPENDIX A Base-Band Pulse Wave forms 78

APPENDIX B Derivation of $p(Z,\phi_1)$ 83

APPENDIX C The Gram-Charlier Expansion 88

REFERENCES 90

LIST OF FIGURES

Figure	Title	Page
2.1	Nonlinear transmission system	8
2.2	Cosine roll off filter transfer function	11
2.3	δ_1 versus BT	12
2.4	δ_2 versus BT	12
2.5	Model for nonlinear channels	14
2.6	Detection system	16
2.7	Vector diagram of received wave and error region	17
3.1	Vector diagram of $u_1(t)$	22
3.2	Symbol error probability for MPSK	28
3.3	Symbol error probability for MPSK	28
3.4	Symbol error probability for BPSK	29
3.5	Symbol error probability for MPSK	29
3.6	Symbol error probability for MPSK	30
3.7	Nonlinear transmission system composed of N bandpass hard-limiters	35
3.8	Symbol error probability for MPSK	38
4.1	Vector diagram of received wave and error region	41
4.2	Symbol error probability for BPSK	49
5.1	Base-band pulse shapes of QPSK, OQPSK, and MSK	54
5.2	Model for hard-limiting satellite system	57
5.3	Vector diagram and error region in hard-limiting satellite system	58
5.4	Bit error probability for QPSK, OQPSK, and MSK	69
5.5	Bit error probability for QPSK, OQPSK, and MSK	69

5.6 Bit error probability for MSK 70
5.7 Bit error probability for MSK 70
5.8 Bit error probability for QPSK 71
5.9 Bit error probability for QPSK 71
5.10 Bit error probability for MSK 72
5.11 Bit error probability for QPSK 72

CHAPTER 1

INTRODUCTION

1.1 Background

Recently an increasing demand of signal transmission in a digital form necessitates the reconsideration of modulation techniques for the efficient utilization of the frequency spectrum. There are three basic modulation techniques : amplitude shift keying (ASK), frequency shift keying (FSK), and phase shift keying (PSK) [1]-[4]. All of these modulations include coherent and noncoherent forms. In system planning,these modulations or the hybrid modulations must be compared, deliberately taking into account of not only Gaussian noise but also other factors that often dominate the system performance. These factors are, for example, intersymbol interference, fading, radio frequency (RF) interference, rainfall attenuation, and/or impulsive noise. In addition, nonlinearities are often included in the transmission system.

In this thesis, the satellite channels are introduced as typical nonlinear channels. In the satellite channels, constant envelope modulations such as FSK and PSK are considered to be more efficient than ASK because the constant envelope modulations are hardly affected by the amplitude nonlinearity. PSK in particular yields an inherently narrow bandwidth and a good error performance. For these reasons, PSK is put into practical use in the satellite channels. In the past several years, the minimum

shift keying (MSK), which is a continuous phase FSK with the modulation index 0.5 [5], has also been expected to yields better performance.

In the satellite channels, there are several features not encountered in terrestrial systems as described below.

(1) THERMAL NOISE IN BOTH LINKS : In the satellite channels the Gaussian thermal noise disturbs the desired signal not only in the up-link but also in the down-link.

(2) INTERSYMBOL AND RF INTERFERENCES : The INTELSAT V system employs four-fold frequency re-use which is performed by use of cross-polarization and spot-beam techniques [6],[7]. This frequency re-use produces an RF interference problem, i.e., adjacent channel and cochannel interferences. The bandwidth of each system is also severly limited to accompany with intersymbol interference. The intersymbol interference and the RF interference problems can easily be the dominant degrading factors, and more important than Gaussian noise in the satellite channels.

(3) SATELLITE TRANSPONDER NONLINEARITIES : On the other hand, the effective use of the amplifier power of the transponder travelling wave tube (TWT) is desired because of the limited TWT power. Especially in a time division multiple access (TDMA) system where one transponder amplifies only one carrier, the operation of the TWT at or near a saturation is inevitable. In this mode of TWT operation, the TWT exhibits the nonlinearities of both AM-AM, and AM-PM conversions [8],[9]. These nonlinearities significantly affect the system performance. In order to compensate for both the AM-AM and AM-PM conversions, a limiter ahead of the TWT is considered to be useful [10]. In satellite systems operating above 10GHz, the limiter is also

effective to overcome rainfall attenuation. For these systems the nonlinearity of the limiter controls the TWT nonlinearities.

The effects of the interferences and nonlinearities are not so difficult to analyze independently. But the analysis methods of a linear channel are not easily extended to a nonlinear channel. The composite problem, that is, the problem of the interferences imposed on the nonlinearities, yields incredible analytical difficulties. In many cases the performance evaluation of nonlinear channels is performed by computer simulations or hard-ware experiments. Therefore a new tool or a new extention of the nonlinear analysis which is mathematically tractable and includes all the dominant factors of the performance degradation is expected to be proposed [11].

1.2 Analysis Methods

As described in Section 1.1, the dominant factors of the performance degradation in the satellite channels are RF interference, intersymbol interference, and the TWT nonlinearities. Much previous work has been devoted to a particular factor or combined factors described above.

First, in a linear channel the RF interference has been frequently assumed identical in effect with that of an equivalent power Gaussian noise. But by accurate analyses [12]-[14], it is shown that this assumption provides a pessimistic estimate for the degradation of the PSK system. In the presence of intersymbol interference, the error probabilities of binary PSK (BPSK) and quarternary PSK (QPSK) can be presented by the direct numeration method [15]. The Chernoff bound or other bounding

techniques have also been introduced for deriving the error probability of PSK [16], and ASK [17]-[19]. If the number of modulating phases M is large, however, both the direct method and the bounding techniques become impractical in computer calculations, inaccurate, or analytically difficult. Therefore, for the accurate estimation of error probability of M-ary PSK (MPSK), the moment space technique based on the superposision principle has been proposed [20]. The moment space technique has been also utilized to evaluate the error probability of PSK [21], [22], ASK [23],[24], and FSK/MSK [25]-[27], considering the combined effects of RF interference and intersymbol interference.

Next in nonlinear channels, intensive studies on PSK system have been done on filtering [28]-[35], TWT back off [28]-[35], high power amplifier (HPA) back off [30], [32], [34], limiters [29], [33],[35], coding [29], [37], RF interferene [28], [32], [33], [36], [37], comparison with MSK or offset QPSK [31]-[33], by computer simulations or laboratory experiments.

On the other hand, due to the complexity of the combined problems of RF interference and intersymbol interference, there has been few general analyses that include all dominant factors of the performance degradation. In mathematical analyses, several types of TWT model have been proposed :

(1) HARD-LIMITER : The hard-limiter is often used in nonlinear analysis because of its analytical facilities. Many works have been devoted to the signal-to-noise power ratio (SNR) [38]-[45], and the SNR improvement at high SNR due to the hard-limiter has been shown in [40]. The output power has been also discussed by using the Complex Fourier Transform [41]-[45]. This method is useful if the Complex Fourier Transform of the nonlinear characteristics is given, but the effects of

intersymbol interference can not be easily included. The expression for the error probability has been presented for BPSK [46], differential PSK (DPSK) [47], [48] and MPSK [49]. In [46] and [49], the comparison with a linear channel has shown the error probability improvement effects due to the hard-limiter. A more general case with the transmission system composed of cascaded hard-limiters [50] has been also considered in [39], [40], [49]. But these works are restricted to the case of only Gaussian noise. The effects of intersymbol interference have been shown only for BPSK [51].

(2) SOFT-LIMITER : It is important to show the effects of the soft-limiter because it is not only more practical than the hard-limiter, but also expected to be used in future systems [10]. In practical systems, the error function type† or piece - wise - linear type limiters has been widely utilized. The piece - wise - linear type limiter has been used for deriving error probability of BPSK in the presence of intersymbol interference [52].

(3) SERIES EXPANSION : A more realistic approximation of TWT operation is performed by the series expansion [8], [53]-[55]. With this method the probability density function (p.d.f.) of the TWT output has been examined in the presence of Gaussian noise, and the error probability of BPSK has been shown by equating undesired componens to Gaussian noise [53]. The effects of RF interference and intersymbol interference have been considered in the analysis of the error probability of QPSK [55]. But

---

† $\mathrm{erf}(x) = \frac{2}{\sqrt{\pi}} \int_0^x \exp(-t^2)\, dt$

the results obtained there for intersymbol interference have been performed by computer simulations.

(4) QUADRATURE MODEL : In the analysis used the quadrature model, the AM-PM conversion is not considered, because it is included in two-quadrature AM-AM conversions. The error probability of BPSK has been derived in a Gaussian noise environment [56]. This quadrature model is also applicable to SNR analysis [57].

(5) VOLTERRA SERIES : In the Volterra series analysis, the nonlinearities and intersymbol interference are treated simultaneously by introducing the Volterra kernels [58]-[61]. The error probability of BPSK and QPSK has been analyzed with the Volterra series in the presence of Gaussian noise [58]. In this analysis, the restriction imposed on the transmit filter needs further extention for practical use.

(6) BARRET RAMPARD EXPANSION : For a Gaussian or multi-carrier input, the Barret Rampard expansion is also useful to analyze the SNR of TWT output signal [62]. But the error probability of PSK has not been presented because of its analytical difficulties.

To show the combined effects of the RF interference and intersymbol interference in the hard-limiting satellite channels, the error probability analysis of QPSK has recently been attempted with the aid of the moment space technique [63]. The obtained expression for the error probability is not a closed form and not mathematically tractable.

In the following chapter, in order to clarify the combined effects of RF interference, intersymbol interference, Gaussian noise, and satellite nonlinearities, a new analytical approach is proposed for obtaining a general expression of the error probability of MPSK.

CHAPTER 2

SYSTEM DESCRIPTION

2.1 Introduction

As typical nonlinear channels, the satellite channels are introduced in this thesis. In relation to the increased importance of the radio frequency (RF) interference problem, the satellite channels are considered to include adjacent and/or cochannel interferences, that is, the band-limited M-ary PSK (MPSK) signal is transmitted through the nonlinear satellite repeater with the disturbances of the narrow band Gaussian noise and RF interference in both up-link and down-link.

In this chapter, an analytical model of the MPSK system in the satellite channels is given, and mathematical representations are expressed for the basic elements used in the analysis which are MPSK signal, intersymbol interference, nonlinear channels including RF interference, and detection scheme.

2.2 Phase Shift Keying Signals

A model for the nonlinear transmission system is shown in Fig.2.1. An MPSK signal $v_0(t)$ is expressed by

$$v_0(t)= \tilde{v}_0(t)\ \exp(j2\pi f_0 t), \qquad (2\text{-}1)$$

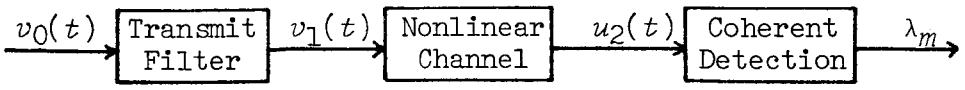

Fig.2.1 Nonlinear transmission system

$$\tilde{v}_0(t)=\sum_{m=-\infty}^{\infty} \mathrm{rect}\{(t-mT)/T\}\ \exp(j2\pi\lambda_m/M), \tag{2-2}$$

where

$$\mathrm{rect}\{t/T\}=\begin{cases} 1, & |t|\leq T/2 \\ 0, & |t|> T/2 \end{cases}, \tag{2-3}$$

$\tilde{v}_0(t)$ denotes the complex envelope† of $v_0(t)$, f_0 is the carrier frequency, T is a symbol duration, and $\lambda_m(=0,1,\ldots M-1)$ is a transmitted message.

2.3 Intersymbol interference

The MPSK signal is band-limited by the transmit filter and accompanied by intersymbol interference. The transmit filter output $\tilde{v}_1(t)$ is represented by

$$\tilde{v}_1(t)=\int_{-\infty}^{\infty} \tilde{v}_0(t)\,\tilde{h}(t-\tau)\,d\tau, \tag{2-4}$$

---

† In what follows, the notation $\tilde{x}$ is used as the complex envelope of x.

where $\tilde{h}(t)$ is a lowpass equivalent impulse responce of the transmit filter. Substituting (2-2) into (2-4), $\tilde{v}_1(t)$ is rewritten as

$$\tilde{v}_1(t) = \sum_{m=-\infty}^{\infty} q(t-mT)\exp(j2\pi\lambda_m/M), \tag{2-5}$$

where

$$q(t) = \int_{-\infty}^{\infty} \mathrm{rect}\{\tau/T\}\,\tilde{h}(t-\tau)\,d\tau. \tag{2-6}$$

Now $\tilde{v}_1(t)$ is decomposed into a desired signal $\tilde{u}_0(t)$ and an intersymbol interference component $\tilde{i}_0(t)$,

$$\tilde{v}_1(t) = \tilde{u}_0(t) + \tilde{i}_0(t), \tag{2-7}$$

where

$$\tilde{u}_0(t) = q(t)\exp(j2\pi\lambda_0/M), \tag{2-8}$$

$$\tilde{i}_0(t) = \sum_{\substack{m=-\infty \\ (m\neq 0)}}^{\infty} q(t-mT)\exp(j2\pi\lambda_m/M). \tag{2-9}$$

In a small time interval, $\tilde{u}_0(t)$ and $\tilde{i}_0(t)$ are regarded to have constant amplitudes, that is

$$\tilde{u}_0(t)\big|_{t\simeq 0} = U_0, \tag{2-10}$$

$$\tilde{i}_0(t)\big|_{t\simeq 0} = I_0\exp(j\psi_0). \tag{2-11}$$

Here $\lambda_0=0$ is assumed without loss of generality under the condition that the transmitted symbol sequence λ_m is equiprobable. U_0, I_0, ψ_0 in (2-10) and (2-11) are derived with the trigonometric sum in (2-8) and (2-9). For adjascent symbols interference ($m=\pm 1$),

$$U_0 = q(0), \tag{2-12}$$

$$I_0 = 2\,q(0)\cos \pi(\lambda_{-1}-\lambda_1)/M, \tag{2-13}$$

$$\psi_0 = \pi(\lambda_{-1} + \lambda_1)/M. \tag{2-14}$$

In this case the phase offset ε due to the intersymbol interference component is given by

$$\varepsilon = \tan^{-1}\left[\frac{I_0 \sin\psi_0}{U_0+I_0\cos\psi_0}\right]. \tag{2-15}$$

In this thesis the cosine roll-off filter is assumed for the transmit filter. Fig.2.2 shows the lowpass equivalent transfer characteristics $\tilde{H}(f)$ of the cosine roll-off filter.

$$\tilde{H}(f) = \begin{cases} \frac{1}{2}\left[1-\sin\left(\frac{\pi|f|}{\eta_R B} - \frac{\pi}{2\eta_R}\right)\right], & \frac{B}{2}(1-\eta_R) \leqq |f| \leqq \frac{B}{2}(1+\eta_R) \\ 1, & 0 < |f| < \frac{B}{2}(1-\eta_R), \\ 0, & \frac{B}{2}(1+\eta_R) < |f| \end{cases} \tag{2-16}$$

where

$$\tilde{H}(f) = \int_{-\infty}^{\infty} \tilde{h}(t) \exp(-j2\pi ft)\, dt \,. \qquad (2\text{-}17)$$

In Fig.2.2, B denotes the 6dB bandwidth, η_R is a roll-off factor, and t_0 is a fixed time delay. Since the fixed time delay does not affect the error performance, $t_0=0$ is assumed in this thesis. For the cosine roll-off filter, the pulse responce $q(t)$ in (2-6) is derived in APPENDIX A.

In order to estimate the amount of intersymbol interference, the desired signal - to - the intersymbol interference component due to the adjacent symbol ($m=\pm 1$) power ratio δ_1, and the desired signal - to - the intersymbol interference componnt due to the symbols of $m=\pm 2$ power ratio δ_2 are calculated for the cosine roll-off filter in Fig.2.4 and Fig.2.5.

$$\delta_1 = q^2(0) \,/\, q^2(\pm T) \qquad (2\text{-}18)$$

$$\delta_2 = q^2(0) \,/\, q^2(\pm T) \qquad (2\text{-}19)$$

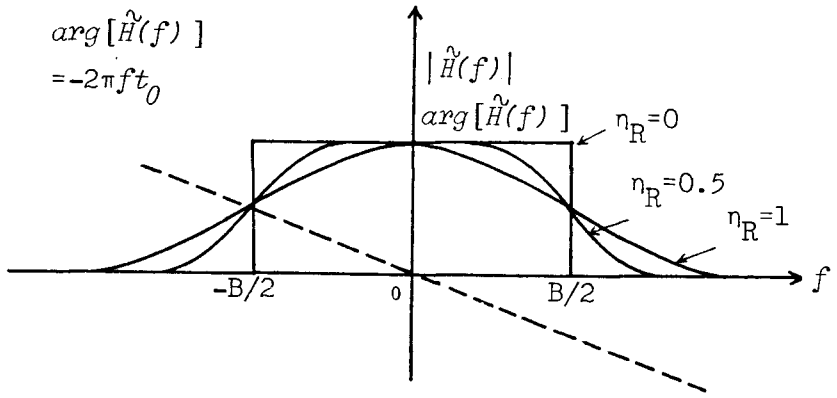

Fig.2.2 Cosine roll off filter transfer function

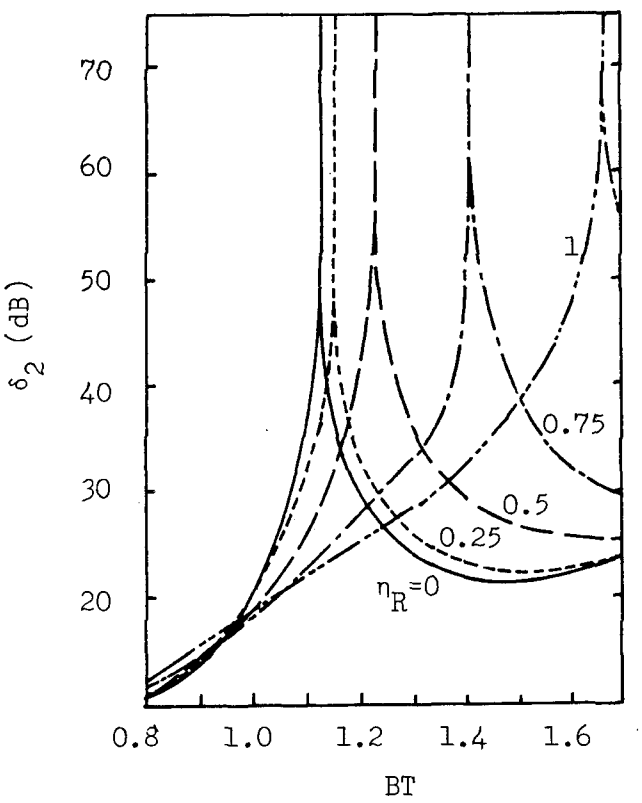

Fig.2.3 δ_1 versus BT

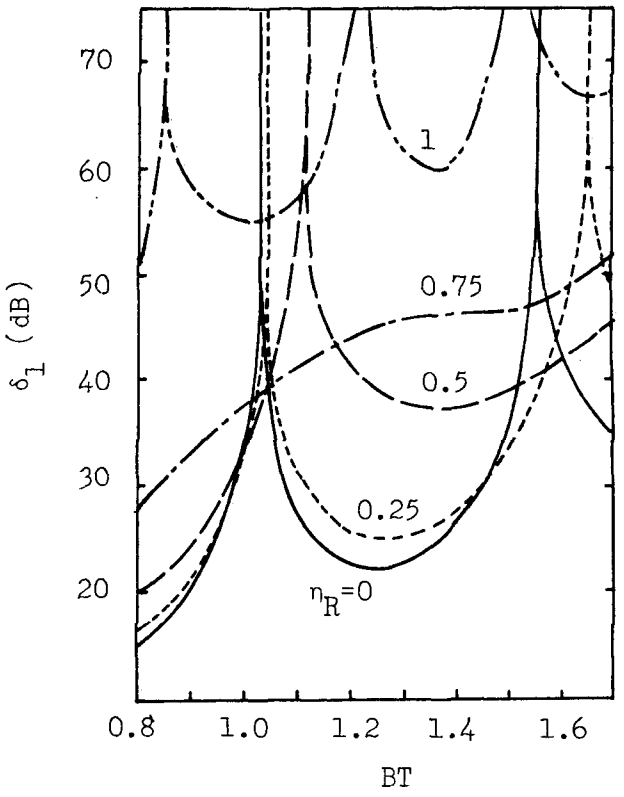

Fig.2.4 δ_2 versus BT

First in Fig.2.3, it is shown that the δ_1 curve for each η_R has a peak at a fixed value of BT. The peak of δ_1 means that the intersymbol interference component due to the adjacent symbols becomes very small at that BT. This peak point is preferable to eliminate the effects of the intersymbol interference component due to the adjacent symbols.

Next Fig.2.4 shows that for the smooth filtering (η_R=1) δ_2 is larger than 50 dB in the region of BT=0.8 - 1.7. In the region of δ_2>50dB the effects of the intersymbol interference component due to the symbols of m=$\pm$2 is considered to be negligible small. So it may concluded that it is sufficient to consider the effects of the intersymbol interference component due to the adjacent symbol for the smooth filtering case in a system analysis.

2.4 Model for Nonlinear Channels

The model for the nonlinear satellite channels is shown in Fig.2.5. The transmit filter output $v_1(t)$ is transmitted via nonlinear satellite repeater with the disturbances of the narrow band Gaussian noise and the interferences in both up-link and down-link.

$$i_k(t)= \sum_{n=1}^{a_k} i_{kn}(t), \quad k=1,2, \tag{2-20}$$

$$i_{kn}(t)= I_{kn} \exp\{j(2\pi f_0 t + \psi_{kn})\}, \quad n=1,2,\cdots,a_k \tag{2-21}$$

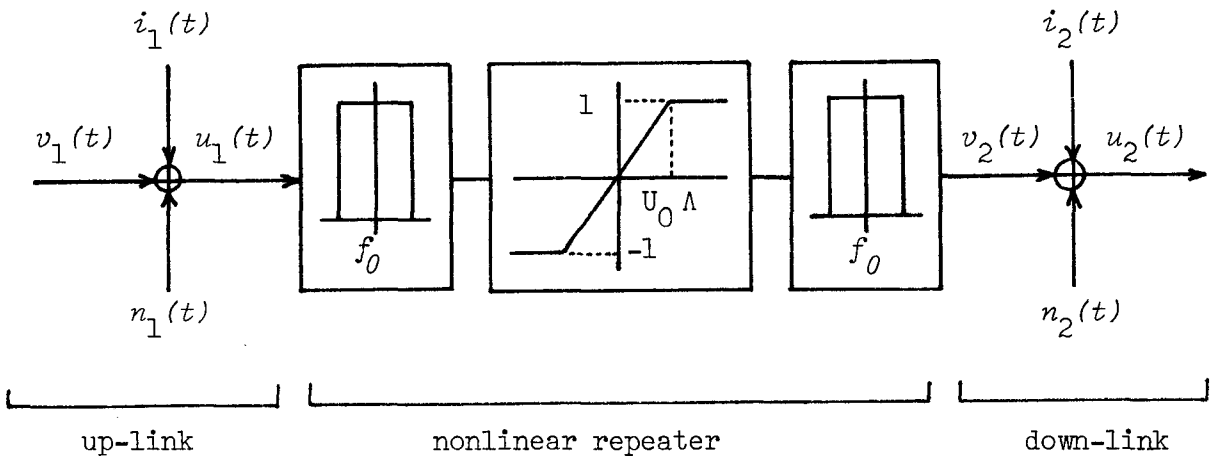

Fig.2.5 Model for nonlinear channels

where subscripts k=1 and k=2 denote the up-link and the down-link respectively, and a_k is the number of interferences in the up-link (k=1) or the down-link (k=2). Each interference has a constant amplitude I_{kn}, and a phase ψ_{kn} which is uniformly destributed on $(0,2\pi)$. These interferences are possibly angle-modulated sinusoidal waves which lie within the bandwidth of the signal.

The narrow band Gaussian noise in the up-link or the down-link is represented by [64]

$$n_k(t) = \tilde{n_k}(t)\ \exp\{j(2\pi f_0 t + \zeta_k(t))\}$$

$$= \{\, n_{ck}(t) + n_{sk}(t)\,\} \exp(j2\pi f_0 t),\ k=1,2, \qquad (2\text{-}22)$$

where $\tilde{n_k}(t)$ has a Rayleigh distribution, and ζ_k is uniformly distributed on $(0,2\pi)$. Also $n_k(t)$, $n_{kc}(t)$, and $n_{ks}(t)$ are the Gaussian random variables with the same power σ_k^2 and mean zero.

The soft-limiter models the satellite transponder which equiped the soft-limiter ahead of the travelling wave tube (TWT) amplifier in order to compensate both AM-AM and AM-PM conversions [10]. In the case of no soft-limiter on board, the soft-limiter also approximates the operation of TWT near a saturation, where the TWT is regarded to have an output of a constant amplitude, and a constant phase which can be compensated at the earth station. The soft-limiter characteristic function is expressed by

$$G(Z) = \begin{cases} Z, & |Z| \le U_0 \\ +1, & Z > U_0 \\ -1, & Z < -U_0 \end{cases}, \qquad (2\text{-}23)$$

where Λ denote the limiting level. $\Lambda=0$ corresponds to a hard-limiter and $\Lambda=\infty$ means a linear amplifier. And U_0 is the amplitude of the desired signal $u_0(t)$ at $t=0$. It is also assumed that the limiter has no phase distortions [10],[41].

2.5 Detection Scheme

A detection system is shown in Fig.2.6. In Fig.2.6, the reeive filter is assumed to be ideal bandpass filter which does not distort the signal. In a coherent detection, the received wave $u_2(t)$ is multiplied by $\cos 2\pi f_0 t$ and $\sin 2\pi f_0 t$ which is assumed to be perfectly recovered in this thesis. Using the outputs of the multipliers, the detector decides the received phase ϕ_2 and announces the transmitted message. A vector diagram of the received wave $u_2(t)$ is shown in Fig.2.7. The transmit filter output $\vec{V_1}$ consists of the desired signal $\vec{U_0}$ and the intersymbol interference component $\vec{I_0}$ with the phase ψ_0. In the up-link,

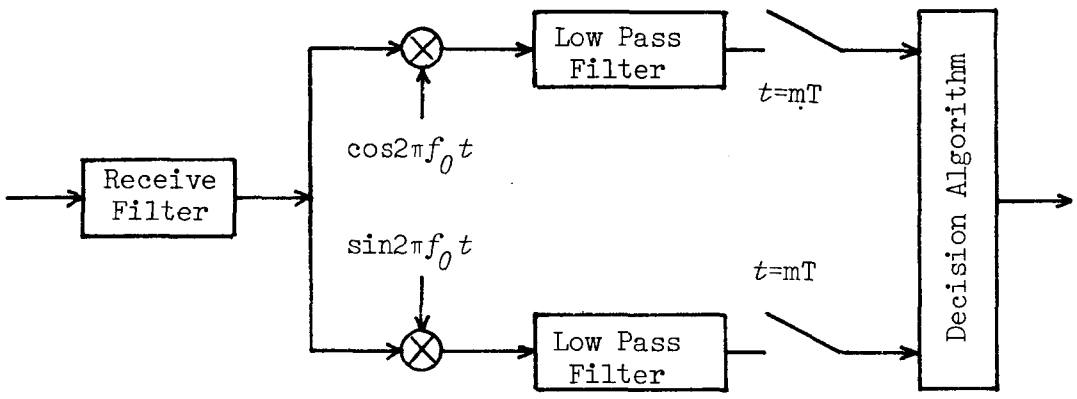

Fig.2.6 Detection system

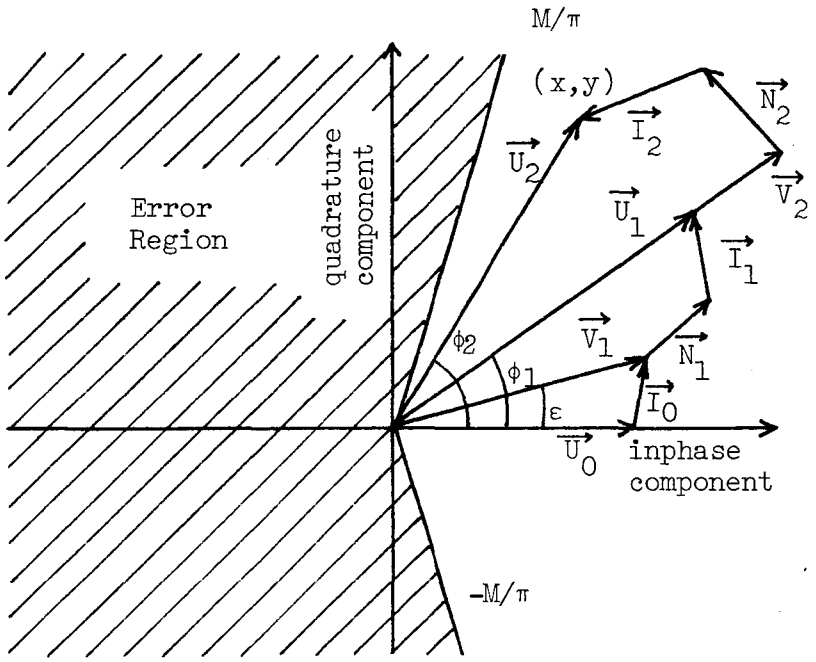

Fig.2.7 Vector diagram of received wave and error region

the narrow band Gaussian noise $\vec{N_1}$ and the multiple RF interferences $\vec{I_1}$ are combined to yield the up-link composite wave $\vec{U_1}$ with a phase ϕ_1. The satellite output $\vec{V_2}$ is also disturbed by the narrow band Gaussian noise $\vec{N_2}$ and the multiple RF interferences $\vec{I_2}$ in the down-link. Then received wave terminates on (x,y).

An error occurs when $\vec{U_2}$ terminates in an error region as shown in Fig.2.7. Therefore the conditional eror probability $Pes|I_0,\psi_0$ of MPSK signal is derived by integrating a probability density function (p.d.f.) $p(\phi_2)$ of the received phase ϕ_2 over the error region in Fig.2.7. Then averaging $Pes|I_0,\psi_0$ with respect to the intersymbol interference component, the desired symbol error probability Pes is obtained.

For a bit error probability analysis in Chapter 5, the error region of $x < 0$ is used. That is, the error region is the same as that of the symbol error probability analysis in binary case.

2.6 Concluding Remarks

In this chapter the system description is given for the PSK signal transmission over the nonlinear channels. As typical nonlinear channels, the satellite channels are introduced, and the mathematical representations of basic elements used in the following chapters are provided.

CHAPTER 3

EFFECTS OF HARD-LIMITING

3.1 Introduction

In digital satellite communications, the power of the satellite travelling wave tube (TWT) is limited, and an operation of TWT at or near a saturation is required for effective utilization of TWT power. The operation at the saturation is modeled by the hard-limiter, because the output of TWT is regarded to consist of a constant amplitude, and a fixed phase delay which can be compensated at the earth station.

For this hard-limiting channel, Cahn has examined the output signal-to-noise power ratio (SNR) of the hard-limiter, and showed the SNR degradation effects at low input SNR [38]. Arastoo, Morinaga, and Namekawa have discussed the cascaded hard-limiters case [40]. Arastoo et al.'s results can be utilized at an arbitrary input SNR case, and both the SNR degradation at low input SNR and the SNR improvements at high input SNR are described.

Mathematical expressions for the error probability of PSK have been derived by Jain and Blackman for binary PSK (BPSK) [46], and by Mizuno, Morinaga, and Namekawa for M-ary PSK (MPSK) [49]. Mizuno, et al.'s results have also included cascaded hard-limiters case. In these works comparisons with a linear channel have been performed, and showed the error probability improvement effects due to the hard-limiter. But these works

have been done in neither the intersymbol interference nor the radio frequency (RF) interference environment. In recent satellite communications, these interference problems become dominant factors of a performance degradation. Ekanayake and Taylor have included only the effects of intersymbol interference in the error probability analysis of BPSK [51]. To discuss the combined effects of the RF interference and the intersymbol interference, Huang, Omura, and Lindsey have presented the error probabilty of quarternary PSK (QPSK) [63]. But the obtained expression is not a closed form and not mathematically tractable.

In this chapter, in the presence of the Gaussian noise in both links, intersymbol interference and RF interference, the probability density function (p.d.f.) of the detected phase is derived for the hard-limiting satellite system, considering intersymbol interference as RF interference. Integrating this p.d.f. over an error region, the error probability of MPSK is obtained. A comparison with the linear channel is made to clarify the error probability improvement effects due to the hard-limiter. Furthermore the effects of cascaded hard-limiters are discussed [65]-[69].

3.2 Probability Density Function of Detected Phase

In order to get the p.d.f. of the detected phase ϕ_2 of the received wave $u_2(t)$, first a p.d.f. of the up-link composite wave $u_1(t)$ is derived. In Fig.3.1, a joint p.d.f. $p(Z,\phi_1)$ is represented by (see APPENDIX B),

$$p(Z,\phi_1) = \sum_{\nu=0}^{\infty} \sum_{\eta=0}^{\infty} \sum_{\ell_{11}=0}^{\infty} \cdots \sum_{\ell_{1a_1}=0}^{\infty} \frac{\varepsilon_\nu}{2\pi} \cos\nu(\phi_1 - \varepsilon)$$

$$\cdot \frac{(-1)^{\ell_{11}+\ell_{12}+\cdots+\ell_{1a_1}+\eta} V_1^{\nu+2\eta}}{2^{2(\ell_{11}+\ell_{12}+\cdots+\ell_{1a_1}+\eta)+\nu} \eta!}$$

$$\cdot \frac{I_{11}^{2\ell_{11}} I_{12}^{2\ell_{12}} \cdots I_{1a_1}^{2\ell_{1a_1}}}{(\ell_{11}!)^2 (\ell_{12}!)^2 \cdots (\ell_{1a_1}!)}$$

$$\cdot \frac{\Gamma(\nu+\eta+\ell_{11}+\ell_{12}+\cdots+\ell_{1a_1}+1)\, Z\, (Z/\sqrt{2}\sigma_1)^\nu}{\Gamma(\nu+1)\,\Gamma(\nu+\eta+1)\, 2(\sigma_1/\sqrt{2})^{\nu+2(\eta+\ell_{11}+\ell_{12}+\cdots+\ell_{1a_1})+2}}$$

$$\cdot {}_1F_1[\,\nu+\eta+\ell_{11}+\ell_{12}+\cdots+\ell_{1a_1}+1;\nu+1;-Z^2/(2\sigma_1^2)\,], \tag{3-1}$$

$$V_1 = U_0 \left(1 + \gamma_0^{-1} + 2\gamma_0^{-\frac{1}{2}} \cos\psi_0\right), \tag{3-2}$$

$$\gamma_0 = U_0^2 / I_0^2, \tag{3-3}$$

where

U_0 : amplitude of the desired signal in (2-12),

I_0 : amplitude of the intersymbol interference component in (2-13),

I_{1n} : amplitude of the up-link n^{th} interference,

σ_1^2 : power of the up-link Gaussian noise,

$\Gamma(\cdot)$: Gamma function,

ε : phase offset due to the intersymbol interference component in (2-15),

γ_0 : the desired signal-to-the intersymbol interference component power ratio.

ψ_0 : phase of the intersymbol interference component in in (2-14),

a_1 : number of the up-link interferences,

${}_1F_1[\cdot;\cdot;\cdot]$: confluent hypergeometric function,

$$\varepsilon_m = \begin{cases} 1, & m=1 \\ 2, & m\neq 1 \end{cases} \quad : \text{Neumann factor.}$$

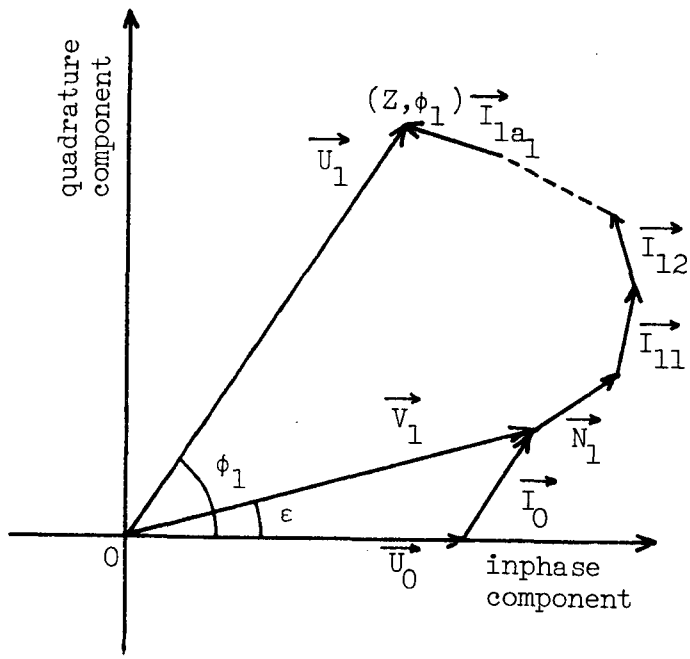

Fig.3.1 Vector diagram of $u_1(t)$

Let start the calculation of $p(\phi)$ with $\nu+\eta+\ell_{11}+\cdots+\ell_{1a_1} \neq 0$ in (3-1). In (3-1), changing the variables as $t=Z^2/2\sigma_1^2$, and using the formula [70,p.280]

$$\int_0^\infty t^{b-1}\ {}_1F_1[a;c;-t]dt=\frac{\Gamma(b)\Gamma(c)\Gamma(a-b)}{\Gamma(a)\Gamma(c-b)} \qquad 0<\mathrm{Re}(b)<\mathrm{Re}(a) \tag{3-4}$$

for averaging $p(Z,\phi_1)$ over Z, then

$$\begin{aligned} p(\phi_1)\Big|_{\nu+\eta+\ell_{11}+\ell_{12}+\cdots+\ell_{1a_1}\neq 0} &= \sum_{\nu=1}^{\infty}\ \sum_{\ell_{11}=0}^{\infty}\ \sum_{\ell_{12}=0}^{\infty}\cdots\sum_{\ell_{1a_1}=0}^{\infty} \frac{\nu}{2\pi}\cos\nu(\phi_1-\varepsilon) \\ &\cdot \frac{(-1)^{\ell_{11}+\ell_{12}+\cdots+\ell_{1a_1}}\ \Gamma(\frac{\nu}{2}+\ell_{11}+\ell_{12}+\cdots+\ell_{1a_1})}{(\ell_{11}!)^2(\ell_{12}!)^2\cdots(\ell_{1a_1}!)^2\ \Gamma(\nu+1)} \\ &\cdot \alpha_1'^{\frac{\nu}{2}+\ell_{11}+\ell_{12}+\cdots+\ell_{1a_1}}\ \gamma_{11}'^{-\ell_{11}}\ \gamma_{12}'^{-\ell_{12}}\cdots\gamma_{1a_1}'^{-\ell_{1a_1}} \\ &\cdot {}_1F_1[\tfrac{\nu}{2}+\ell_{11}+\ell_{12}+\cdots+\ell_{1a_1};\nu+1;-\alpha_1']. \end{aligned} \tag{3-5}$$

where

α_1' $(=V_1^2/2\sigma_1^2)$: effective up-link carrier-to-noise power ratio (CNR),

γ_{1n}' $(=V_1^2/2I_{1n}^2)$: effective carrier-to-interference power ratio (CIR) of up-link n^{th} interference.

α_1' and γ_{1n}' can be rewritten with the relation of (3-2).

$$\alpha_1' = \alpha_1 \left(1 + \gamma_0^{-1} + 2\gamma_0^{-\frac{1}{2}} \cos\psi_0 \right) \tag{3-6}$$

$$\gamma_{1n}' = \gamma_{1n} \left(1 + \gamma_0^{-1} + 2\gamma_0^{-\frac{1}{2}} \cos\psi_0 \right) \tag{3-7}$$

When $\nu+\eta+\ell_{11}+\cdots+\ell_{1a_1}=0$, from (3-1)

$$p(Z,\phi_1) = \frac{Z}{2\pi\sigma_1^2} \; {}_1F_1\left[1;1;-\frac{Z^2}{2\sigma_1^2}\right] \tag{3-8}$$

In (3-6), changing the variables as $t=Z^2/2\sigma_1^2$, and averaging $p(Z,\phi_1)$ over Z with the relationship [42,p.1074]

$${}_1F_1[a;a;-x] = \exp(-x) \tag{3-9}$$

yields

$$p(\phi_1)\Big|_{\nu+\eta+\ell_{11}+\ell_{12}+\cdots+\ell_{1a_1}=0} = \frac{1}{2\pi} \tag{3-10}$$

Therefore, from (3-5) and (3-10), $p(\phi_1)$ is derived with

$$\begin{aligned} p(\phi_1) = {} & p(\phi_1)\Big|_{\nu+\eta+\ell_{11}+\ell_{12}+\cdots+\ell_{1a_1}\neq 0} \\ & + p(\phi_1)\Big|_{\nu+\eta+\ell_{11}+\ell_{12}+\cdots+\ell_{1a_1}=0} \end{aligned} \tag{3-11}$$

$$p(\phi_1) = \frac{1}{2\pi} + \sum_{\nu=1}^{\infty} \frac{\nu}{2\pi\Gamma(\nu+1)} \cos\nu(\phi_1-\varepsilon) \, f_1(\nu) \tag{3-12a}$$

$$f_1(\nu) = \sum_{\ell_{11}=0}^{\infty} \sum_{\ell_{12}=0}^{\infty} \cdots \sum_{\ell_{1a_1}=0}^{\infty} \alpha_1'^{\frac{\nu}{2}+\ell_{11}+\ell_{12}+\cdots+\ell_{1a_1}}$$

$$\cdot \frac{(-1)^{\ell_{11}+\ell_{12}+\cdots+\ell_{1a_1}}}{(\ell_{11}!)^2(\ell_{12}!)^2\cdots(\ell_{1a_1}!)^2} \gamma_{11}'^{-\ell_{11}} \gamma_{12}'^{-\ell_{12}} \cdots \gamma_{1a_1}'^{-\ell_{1a_1}}$$

$$\cdot \Gamma\left(\frac{\nu}{2}+\ell_{11}+\ell_{12}+\cdots+\ell_{1a_1}\right) {}_1F_1\left[\frac{\nu}{2}+\ell_{11}+\ell_{12}+\cdots+\ell_{1a_1};\nu+1;-\alpha_1'^2\right] \tag{3-12b}$$

Note that the p.d.f. (3-12) becomes the Middleton's results [42, p.417] with eliminating the parameters of intersymbol interference and interference, i.e., $I_0=0$, $I_{1n}=0$, $\psi_0=0$.

Since the phase ϕ_2 of $u_2(t)$ is generally the composite phase of the angle-modulated signal $v_2(t)$, the down-link Gaussian noise $n_2(t)$, and the down-link interferences $i_2(t)$, its conditional p.d.f. $p(\phi_2|\phi_1)$ can be derived by eliminating the parameters of the intersymbol interference component in (3-12).

$$p(\phi_2|\phi_1) = \frac{1}{2\pi} + \sum_{\nu=1}^{\infty} \frac{\nu}{2\pi\Gamma(\nu+1)} \cos\nu(\phi_1-\phi_2)\, f_2(\nu) \tag{3-13a}$$

$$f_2(\nu) = \sum_{\ell_{21}=0}^{\infty} \sum_{\ell_{22}=0}^{\infty} \cdots \sum_{\ell_{2a_2}=0}^{\infty} \alpha_2^{\frac{\nu}{2}+\ell_{21}+\ell_{22}+\cdots+\ell_{2a_2}}$$

$$\cdot \frac{(-1)^{\ell_{21}+\ell_{22}+\cdots\ell_{2a_2}}}{(\ell_{21}!)^2(\ell_{22}!)^2\cdots(\ell_{2a_2}!)^2} \gamma_{21}^{-\ell_{21}} \gamma_{22}^{-\ell_{22}} \cdots \gamma_{2a_2}^{-\ell_{2a_2}}$$

$$\cdot \Gamma\left(\frac{\nu}{2}+\ell_{21}+\ell_{22}+\cdots+\ell_{2a_2}\right) {}_1F_1\left[\frac{\nu}{2}+\ell_{21}+\ell_{22}+\cdots+\ell_{2a_2};\nu+1;-\alpha_2^2\right] \tag{3-13b}$$

where

α_2 : down-link CNR

γ_{1i} $(i=1,2,\ldots,a_2)$: CIR of down-link i^{th} interference.

Hence the p.d.f. $p(\phi_2)$ of the received wave $u_2(t)$ is obtained with the convolution as [74]

$$p(\phi_2) = \int_0^{2\pi} p(\phi_2|\phi_1)\, p(\phi_1)\, d\phi_1 \tag{3-14}$$

Substituting (3-12) and (3-13) into (3-14) and using the trigonometric relation [42,p.1081]

$$\int_0^{2\pi} \cos m(\theta+\eta)\cos n(\theta+\gamma)\, d\theta = \frac{2\pi}{\varepsilon_m}\,\delta_{mn}\cos m(\eta-\gamma) \tag{3-15}$$

$$\begin{cases} \varepsilon_0=1 \\ \varepsilon_m=2 \quad (m\neq 0) \end{cases} \qquad \begin{cases} \delta_{mn}=1 \quad (m\neq n) \\ \delta_{mn}=0 \quad (m\neq n) \end{cases},$$

Finally the desired result $p(\phi_2)$ is obtained by

$$p(\phi_2) = \frac{1}{2\pi} + \sum_{\nu=1}^{\infty} \frac{\nu^2}{4\pi\,\Gamma(\nu+1)} \cos\nu(\phi_2-\varepsilon)\; f_1(\nu)\, f_2(\nu) \tag{3-16}$$

where $f_1(\nu)$=(3-12b), and $f_2(\nu)$=(3-13b).

3.3 Error Probability

The error occurs when the received phase ϕ_2 lies outside the region $[\pi/M,-\pi/M]$ in Fig.2.7. Therefore by integrating (3-16) over the error region, the conditional error probability $Pes|I_0,\psi_0$ of MPSK signal transmitted via the hard-limiter becomes

$$Pes|I_0,\psi_0 = 1 - \int_{-\pi/M}^{\pi/M} p(\phi_2)\, d\phi_2 . \tag{3-17}$$

Since this integral is simply performed on $\cos\nu(\phi_2-\varepsilon)$ in (3-16), the conditional error probability $Pes|I_0,\psi_0$ is represented by

$$Pes|I_0,\psi_0 = 1 - \frac{1}{M} - \sum_{\nu=1}^{\infty} \frac{\nu}{2\pi\,\Gamma^2(\nu+1)} \sin(\nu\pi/M)\,\cos\nu\varepsilon\; f_1(\nu)\, f_2(\nu) \tag{3-18}$$

where $f_1(\nu)$ =(3-12b) and $f_2(\nu)$ =(3-13b). Including the intersymbol interference component due to adjacent symbols, the condition I_0,ψ_0 in (3-18) can be rewritten with the symbol pattern λ_{-1} ,λ_0 ,λ_1 . Therefore the average error probability Pes is expressed by.

$$Pes = \frac{1}{M^2} \sum_{\lambda_{-1}=0}^{M-1} \sum_{\lambda_1=0}^{M-1} Pes|\lambda_{-1},\lambda_0,\lambda_1 . \tag{3-19}$$

The numerical results of the error probability (3-19) are shown by the solid lines in Figs.3.2-3.6.

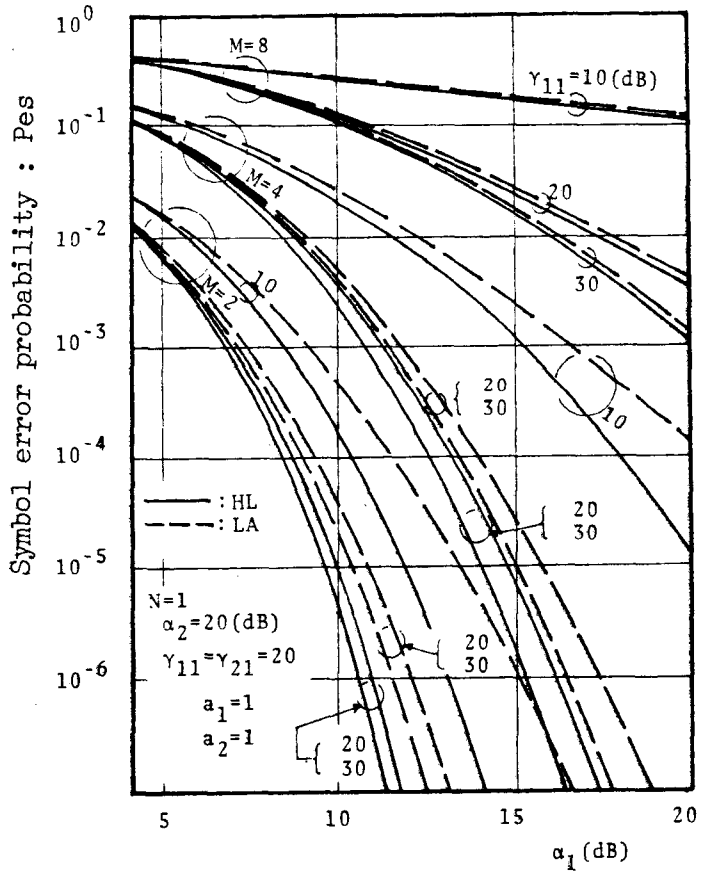

Fig.3.2 Symbol error probability for MPSK
(up-link,down-link : one interference + noise)

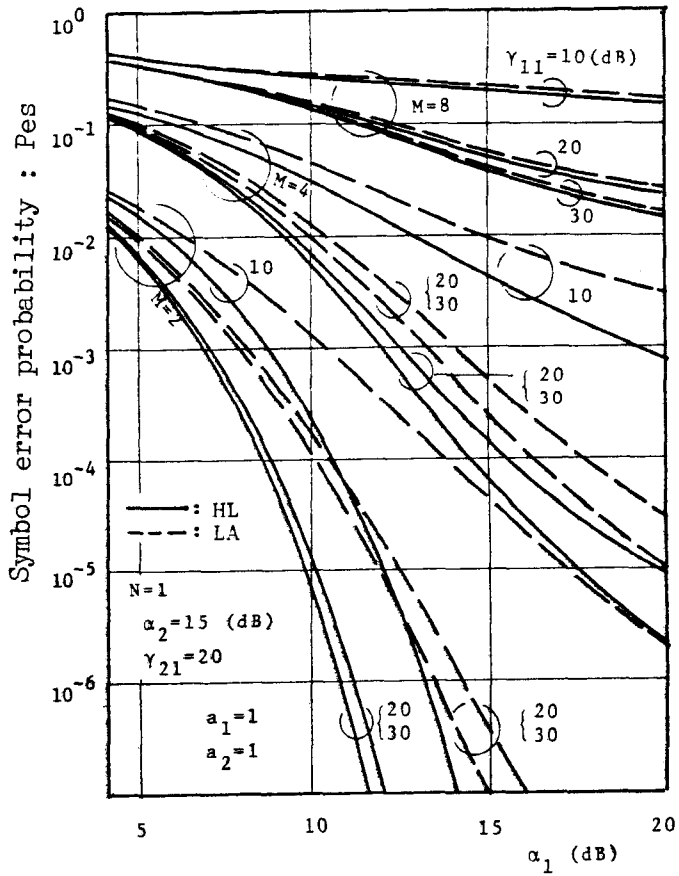

Fig.3.3 Symbol error probability for MPSK
(up-link, down-link : one interference + noise)

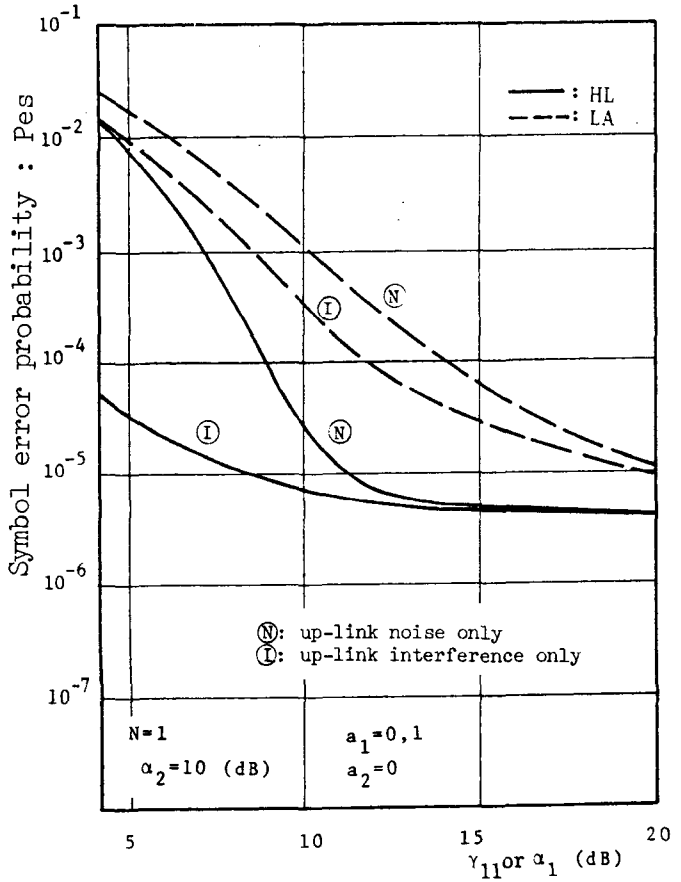

Fig.3.4 Symbol error probability for BPSK

(up-link : noise or one interference, down-link : noise only)

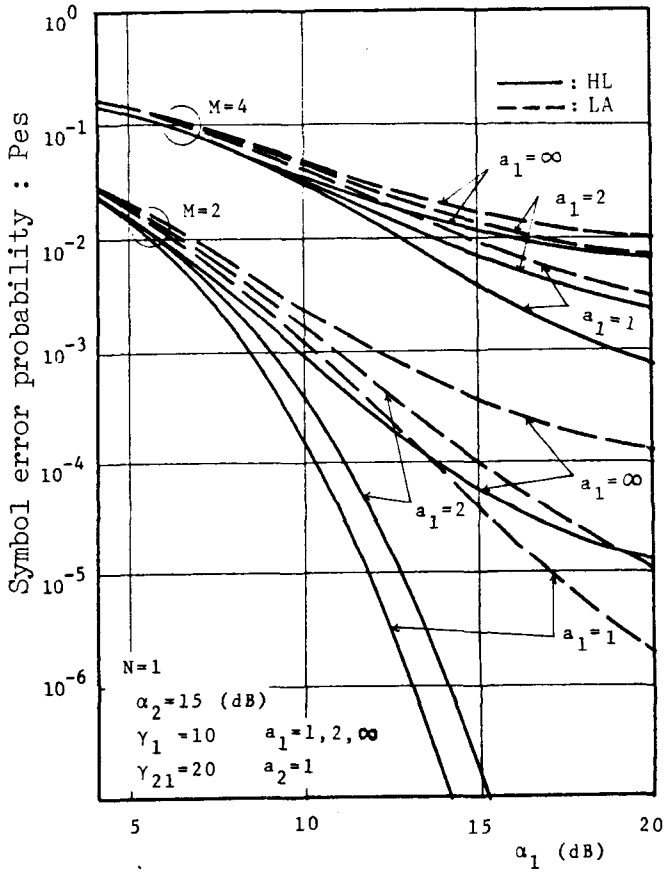

Fig.3.5 Symbol error probability for MPSK

(up-link : multiple interference + noise, down-link : one interference + noise)

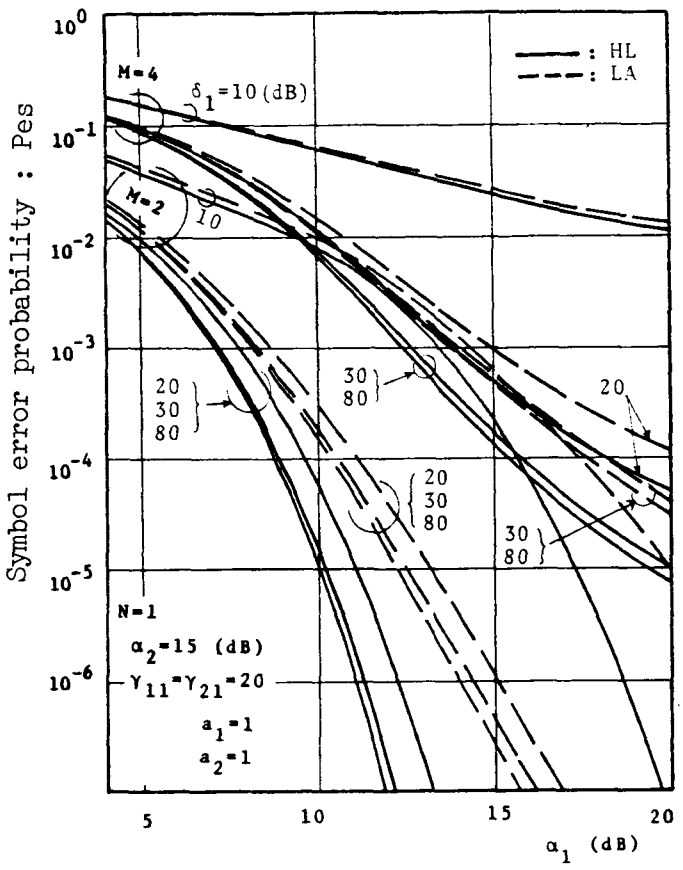

Fig.3.6 Symbol error probability for MPSK
(up-link, down-link : one interference + noise)

3.4 Comparison with Linear Channel

In this section the error probability of MPSK signal in a linear channel is considerd. In the linear channel the transmission system has a linear amplifier instead of the hard-limiter in Fig.2.5. The nonliniar system is compared with

the linear amplifier (LA) system under the condition of the same out put power for both systems.

Let the average power of the up-link composite wave be P_U :

$$P_U = P_{TU} + P_{NU} + P_{IU} \quad , \tag{3-20}$$

where

P_{TU} $(=U_0^2/2+I_0^2/2+U_0I_0\cos\psi_0)$: transmitter output power,
P_{NU} $(=\sigma_1^2)$: power of up-link noise,
P_{IU} $(=I_{11}^2/2+I_{12}^2/2+\ldots+I_{1a_1}^2/2)$: total power of up-link interferences.

Then the total average power P_C of the LA output, which is identical with the hard-limiter output power, is a sum of the transmitter output component P_{TC} , the noise component P_{NC} , and the interference component P_{IC} :

$$P_C = P_{TC} + P_{NC} + P_{IC} \tag{3-21}$$

$$P_{TC}=P_C \cdot P_{TU}/P_U \tag{3-22}$$

$$P_{NC}=P_C \cdot P_{NU}/P_U \tag{3-23}$$

$$P_{IC}=P_C \cdot P_{IU}/P_U \tag{3-24}$$

Furthermore, noise $n_2(t)$ and interference $i_2(t)$ are added to the LA output in the down-link. Hence the CNR α^L at the receiver is given by

$$\alpha^{L} = \frac{P_{TC}}{P_{NC}+\sigma_2^2} = \frac{\alpha_1'\alpha_2}{1+\alpha_1'+\alpha_2+\alpha_1'(\gamma_{11}'^{-1}+\gamma_{12}'^{-1}+\cdots+\gamma_{1a_1}'^{-1})} \tag{3-25}$$

where

α_1' : effective up-link CNR,

α_2 : down-link CNR,

γ_{1n}' $(n=1,2,\ldots,a_1)$: effective CIR of up-link n^{th} interference.

The CIR $\gamma_{1n}'^{L}$ of the up-link interference is the same as :

$$\gamma_{1n}'^{L} = \gamma_{1n}' \quad (n=1,2,\cdots,a_1). \tag{3-26}$$

and the CIR γ_{2i}^{L} of the down-link interferences is :

$$\gamma_{2i}^{L} = \frac{P_{TC}}{I_{2i}^2/2} = \frac{\gamma_{2i}}{1+\alpha_1^{-1}+(\gamma_{11}'^{-1}+\gamma_{12}'^{-1}+\cdots+\gamma_{1a_1}'^{-1})} \quad (i=1,2,\cdots,a_2), \tag{3-27}$$

The p.d.f. of the received phase in the LA system is therefore obtained from (3-12) by using α^{L} instead of α_1' in (3-12b) and substituting both $\gamma_{1n}'^{L}$, $n=1,2,\ldots,a_1$, for γ_{1n}' in (3-12b), and γ_{2i}^{L}, $i=1,2,\ldots,a_2$, for γ_{1n}' in (3-12b), taking note that the number of interferences increases a_1+a_2 in total. Therefore the conditional error probability of the MPSK signal in the linear channel can be derived by integrating $p(\phi_1)$ over the

error region. Then the average error probability is obtained by averaging the conditional error probability with respect to symbol pattern. The numerical results for the LA system, as well as for the hard-limiting (HL) system, are shown in Figs.3.2-3.6. The effect of intersymbol interference is included only in Fig.3.6.

In Figs.3.2-3.6, it is shown that the HL system yields better performance than the LA system for almost all practical values of CNR and CIR. However, the region of low CNR and/or CIR (say less than 0dB), for which no numerical results are given in those figures, it may be guessed that the error probability of the HL system becomes worse than that of the LA system by the small signal suppression effects of HL. The error probability improvements of the HL system become less significant as the number of modulating phases increases. For example, In Fig.3.3 for BPSK at γ_{11}=10dB, the required CNR of the HL system to achieve Pes=10^{-5} is 2.5dB less than that of LA system. Therefore at this point the HL system has a 2.5dB noise margin. But in Fig.3.2 for QPSK at γ_{11}=20dB, this margin decreases 1.0dB. The same tendency is observed from the view point of the interference margin. In Fig.3.3, it is seen that there is a region in which the error probability for the HL system at γ_{11}=10dB is better than that for the LA system at γ_{11} =20dB in BPSK. In such a region the HL system has a remarkable interference margin (more than 20dB), and similarly in QPSK the interference margin is more than 10dB. However, in the octonary PSK the HL system has has no significant inprovements.

Now error probability improvements of the HL system are examined under the up-link noise limited or the up-link interference limited case. It is assumed that in the up-link

either noise or interference exists. In Fig.3.4, (N) denotes an error probability for the up-link noise limited case and (I) denotes an error probability for the up-link interference limited case. It is found from this figure that the error probability improvement of the HL system for the up-link interference-limited case is larger than that for the up-link noise limited. For example, for Pes=10^{-5} the HL system has a 12dB interference margin in (I) and a 9dB noise margin in (N) compared with the LA system.

Fig.3.5 shows the error probabilities in the presence of multiple up-link interferences under the condition that the carrier-to-total interferences power ratio γ_1 is fixed to 10dB. It is seen that the error probability depends severely on the number of interferences a_1 and that the noise-like interference case ($a_1=\infty$) causes the worst error probability. For such a noise-like interference case (i.e., for large a_1, say, over four), simplification in computing the error probability may be made possible by equating with Gaussian noise and by using the central limit theorem [71].

Fig.3.6 shows the error probability of MPSK in the presence intersymbol interference due to adjacent symbols. In Fig.3.6 δ_1 is the parameter of intersymbol interference in (2-18). The parameters BT and η_R of the transmit filter for each δ_1 are shown in Fig.2.3. It is shown that the error probability becomes worse according to the amount of intersymbol interference, but the error probability improvements become more significant in the presence of intersymbol interference.

3.5 Effects of Cascaded Hard-Limiters

A transmission system with cascaded hard-limiters is shown in Fig.3.7. The composite wave $u_k(t)$ in the k^{th} -link (k=1,2,...,N+1) consists of the signal $v_k(t)$, a narrow band Gaussian noise $n_k(t)$ with mean zero variance σ_k^2, and multiple interferences $i_k(t)$:

$$u_k(t) = v_k(t) + n_k(k) + i_k(t) \qquad k=1,2,\ldots,N+1 \qquad (3\text{-}28)$$

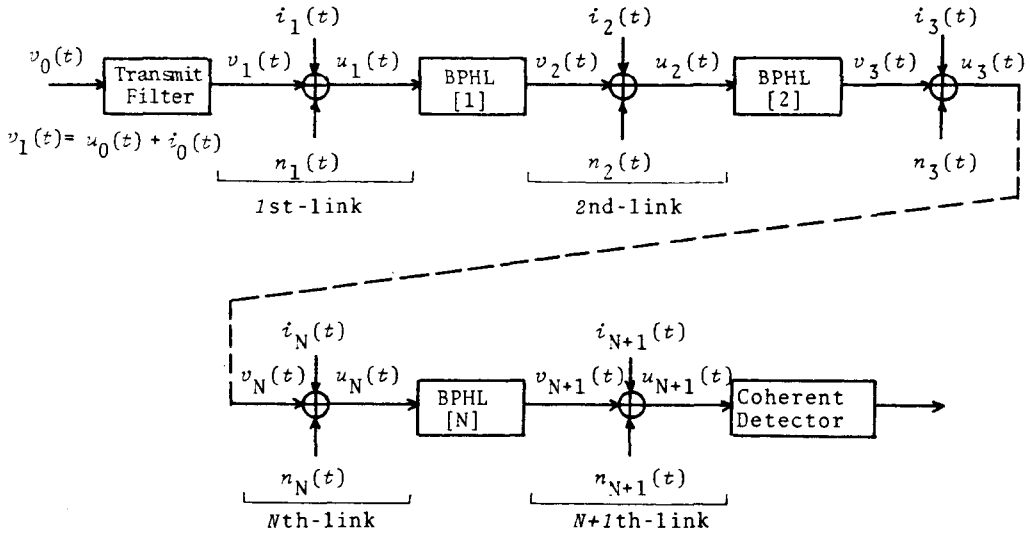

Fig.3.7 Nonlinear transmission system composed of N bandpass hard-limiters

$$i_k(t) = \sum_{n=1}^{a_k} i_{kn}(t) \tag{3-29}$$

$$i_{kn}(t) = I_{kn} \exp\{j(2\pi f_0 t + \psi_{kn})\},\ n=1,2,\cdots,a_k \tag{3-30}$$

where I_{kn} is a constant amplitude, and the phase ψ_{kn} is uniformly distributed on $[0,2\pi]$. Note that $u_k(t)$ for $1\le k\le N$ shows the input to the k^{th}-stage band pass hard-limiter (BPHL)[k] and $u_{N+1}(t)$ shows the input to the final coherent detector. Then the output signal $v_{k+1}(t)$ of BPHL[k] has a constant amplitude and the same phase as that of the input $u_k(t)$ to BPHL[k], k=1,2,...,N, where each BPHL output power level may be chosen arbitrary, i.e., for this analysis only CNR and CIR are required. In the receiver $u_{N+1}(t)$ is coherently demodulated to get the message.

As well as the derivation of $p(\phi_2|\phi_1)$ in Section 3.3 the conditional p.d.f. $p(\phi_k|\phi_{k-1})$ is represented by

$$p(\phi_k|\phi_{k-1}) = \frac{1}{2\pi} + \sum_{\nu=1}^{\infty} \frac{\nu}{\pi\,\Gamma(\nu+1)} \cos\nu(\phi_k-\phi_{k-1})\, f_k(\nu) \tag{3-31a}$$

$$f_k(\nu) = \sum_{\ell_{k1}=0}^{\infty} \sum_{\ell_{k2}=0}^{\infty} \cdots \sum_{\ell_{ka_k}=0}^{\infty} \alpha_k^{\frac{\nu}{2}+\ell_{k1}+\ell_{k2}+\cdots+\ell_{ka_k}} \cdot \frac{(-1)^{\ell_{k1}+\ell_{k2}+\cdots+\ell_{ka_k}}}{(\ell_{k1}!)^2(\ell_{k2}!)^2\cdots(\ell_{ka_k}!)^2} \gamma_{k1}^{-\ell_{k1}} \gamma_{k2}^{-\ell_{k2}} \cdots \gamma_{ka_k}^{-\ell_{ka_k}}$$

$$\cdot \Gamma\left(\frac{\nu}{2}+\ell_{k1}+\ell_{k2}+\cdots+\ell_{ka_k}\right)\, {}_1F_1\left[\frac{\nu}{2}+\ell_{k1}+\ell_{k2}+\cdots+\ell_{ka_k};\ \nu+1;\ -\alpha_k^2\right] \tag{3-31b}$$

where

α_k : k^{th}-link CNR,

γ_{kn} : CIR of k^{th}-link n^{th} interference,

a_k : number of k^{th}-link interferences.

The p.d.f. $p(\phi_{N+1})$ of the received phase ϕ_{N+1} is obtained by an N-fold convolution as

$$p(\phi_{N+1}) = \int_0^{2\pi}\int_0^{2\pi}\cdots\int_0^{2\pi} p(\phi_{N+1}|\phi_N)\cdots p(\phi_2|\phi_1)p(\phi_1)\, d\phi_1 d\phi_2\cdots d\phi_N. \tag{3-32}$$

With the relation of (3-15), $p(\phi_{N+1})$ is derived as

$$p(\phi_{N+1}) = \frac{1}{2\pi} + \sum_{\nu=1}^{\infty} \frac{\nu^{N+1}}{2^{N+1}\pi\, \Gamma^{N+1}(\nu+1)} \cos\nu(\phi_{N+1}-\varepsilon) \prod_{k=1}^{N+1} f_k(\nu), \tag{3-33}$$

where $f_1(\nu)$=(3-12b), and $f_k(\nu)$=(3-31b), k=2,3,...,N+1.

The conditional error probability of the MPSK signal through the N-cascaded BPHL system is derived by integrating $p(\phi_{N+1})$ over the error region in Fig.2.7.

$$Pes|I_0,\psi_0 = 1 - \frac{1}{M} - \sum_{\nu=1}^{\infty} \frac{\nu^N}{2^N \pi\, \Gamma^{N+1}(\nu+1)} \sin(\nu\pi/M)$$

$$\cdot \cos\nu\varepsilon \prod_{k=1}^{N+1} f_k(\nu) \tag{3-34}$$

The average error probability Pes is obtained by averaging $Pes|I_0,\psi_0$ over the symbol pattern. For example, including intersymbol interference due to adjacent symbols

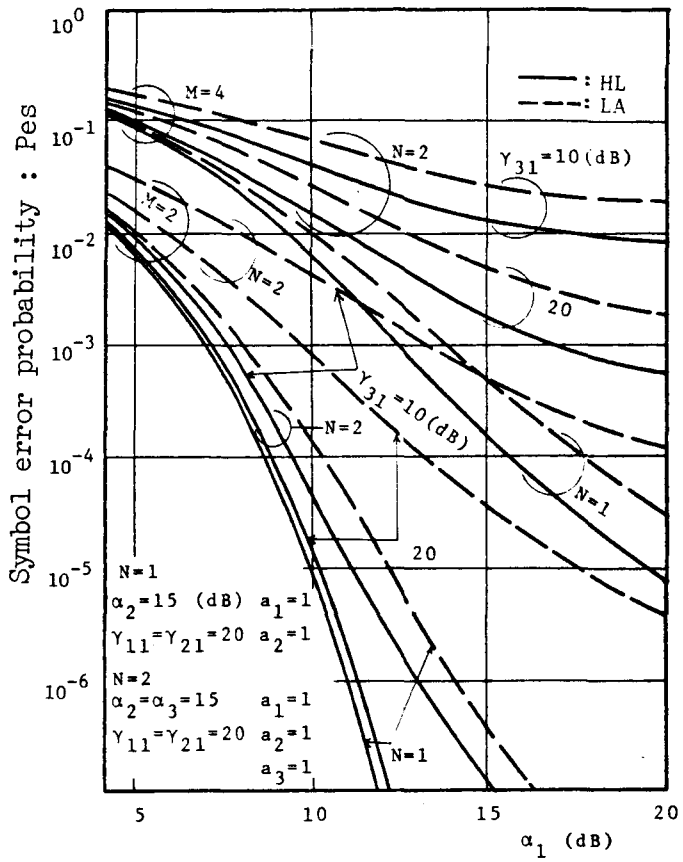

Fig.3.8 Symbol error probability for MPSK (first, second, third-link : one interference + noise)

(3-19) is utilized to get the average error probability.

From (3-34), (3-12b), and (3-31b), it is found that in the absence of intersymbol interference the error probability of the N-cascaded HL system is symmetric about links†, i.e., the same error probability is obtained even if the parameters of one link are exchanged for those of another link. The numerical

---

† In the presence of intersymbol interference, this symmetrisity is also present without first-link.

results for N=1, and N=2 in the absence of intersymbol interfrence are shown by the solid lines in Fig.3.8. In a similar manner to the analysis of Section 3.4, the error probability of the cascaded LA system is calculated in Fig.3.8 under the condition that each LA has the same output power as HL system.

Note that the increase of the number of HL's does not significantly degrade the error probability compared to the case in the LA system.

3.6 Concluding Remarks

In this chapter the effects of hard-limiting on MPSK are discussed in the presence of intersymbol interference, RF interference, and Gaussian noise. Considering intersymbol interference as RF interference, the p.d.f. of the detected phase is derived. Integration this p.d.f. over the error region yields the error probability. A comparison with the linear channel is performed in order to clarifying the effects of the hard-limiter. Numerical results show that the HL system has the noise suppression, the intersymbol interference suppression, and RF interference suppression effects. The error probability of N-cascaded hard-limiter system is also discussed.

CHAPTER 4

EFFECTS OF SOFT-LIMITING

4.1 Introduction

The soft-limiter can model not only more practically the travelling wave tube (TWT) than the hard-limiter, but also precisely the new systems [10],[29],[35] which provide the limiter on board. Sato and Mizuno introduced a soft-limiter with a linearlizer [10]. It was equipped ahead of the TWT in order to overcome the TWT nonlinearity and radio frequency (RF) interference. They showed that this device yielded significant interference immunity effects in phase shift keying (PSK) signal transmission by a INTELSAT V simulator. The soft-limiter is expected to be one of the effective models for the TWT in future satellite systems.

For this soft-limiting channel, there are few studies on analytical methods. For example, Ekanayake and Taylor have analyzed the binary PSK (BPSK) error probability in the soft-limiting channel using the moment space technique [52]. But this work does not consider the influences of RF interference and the limiting level of the soft-limiter.

In this chapter, the effects of the soft-limiter in interference environment is discussed. Using the joint probability density function (p.d.f.) of the up-link composite wave, the p.d.f. of the receiver input wave is derived with the aid of the Gram - Charlier expansion. Through this p.d.f., the

error probability is obtained to show the system performances. Also comparisons with the hard-limiting channel and the linear channel are done in order to clarify the effect of the soft-limiter [72],[73].

4.2 Probability Density Function of Detected Amplitude

In this section the moments of the satellite output $v_2(t)$ and the down-link disturbances $n_2(t)+i_2(t)$ is derived in order to obtain the moments of the received input wave $v_2(t)+n_2(t)+i_2(t)$. Using these moments, the p.d.f. of $u_2(t)$ is obtained with the aid of the Gram - Charlier expansion.

(1) Moments of $v_2(t)$

The vector diagram of the receiver input wave $u_2(t)$ is shown in Fig.4.1. The up-link composite wave $u_1(t)$ is represented by

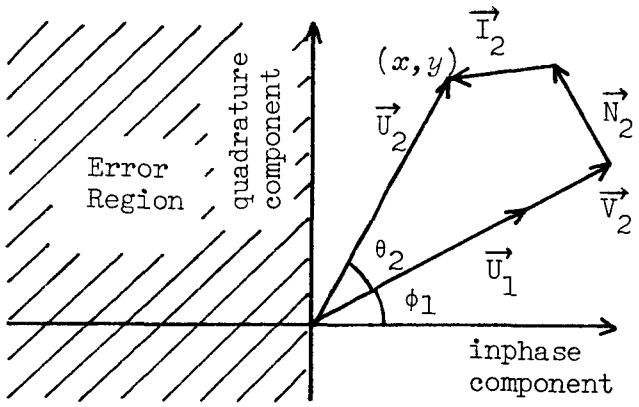

Fig.4.1 Vector diagram of received wave and error region

$$u_1(t) = u_0(t) + i_0(t) + n_1(t) + i_1(t), \tag{4-1}$$

where

$u_0(t)$: desired BPSK signal in (2-10),
$i_0(t)$: intersymbol interference component in (2-11),
$n_1(t)$: up-link Gaussian noise in (2-22),
$i_1(t)$: up-link RF interference in (2-20).

Here the number of up-link interferences is assumed to be one (a_1=1). Using $p(Z,\phi_1)$ in (3-1) and $G(Z)$ in (2-23), The q^{th} moment $m_U(q)$ of the inphase component of $v_2(t)$ is obtained as

$$m_U(q) = \int_0^{U_0\Lambda} \int_0^{2\pi} \left(\frac{Z}{U_0\Lambda}\right)^q \cos^q\phi_1 \, p(Z,\phi_1) \, d\phi_1 dZ$$

$$+ \int_{U_0\Lambda}^{\infty} \int_0^{2\pi} \cos^q\phi_1 \, p(Z,\phi_1) \, d\phi_1 \, dZ \, . \tag{4-2}$$

For convenience, (4-2) is decomposed as

$$m_U(q) = s_1(q) + s_2(q). \tag{4-3}$$

where

$$s_1(q) = \int_0^{\infty} \int_0^{2\pi} \cos^q\phi_1 \, p(Z,\phi_1) \, d\phi_1 \, dZ \, , \tag{4-4}$$

$$s_2(q) = \int_0^{U_0\Lambda} \int_0^{2\pi} \{(\frac{Z}{U_0\Lambda})^q - 1\} \cos^q\phi_1 \; p(Z,\phi_1) \; d\phi_1 \, dZ \; . \qquad (4\text{-}5)$$

Note that $s_1(q)$ is due to the hard-limiting component of $G(Z)$, and $s_2(q)$ denotes the non- hard-limiting component of $G(Z)$. First using $p(\phi_1)$ in (3-12), $s_1(q)$ is rewritten with the equation of

$$\frac{1}{2\pi} \int_0^{2\pi} \cos^n\phi \; \cos m(\phi + \varepsilon) \; d\phi$$

$$= \begin{cases} \dfrac{n!}{2^n \, (\frac{n-m}{2}!)(\frac{n+m}{2}!)} \cos m\varepsilon, & \dfrac{n-m}{2} : \text{non-negative integer} \\ 0, & \dfrac{n-m}{2} : \text{otherwise} \end{cases} \qquad (4\text{-}6)$$

to get

$$s_1(q) = \sum_{\substack{\nu=0 \\ (2\nu \neq q)}}^{[q/2]} \sum_{\ell=0}^{\infty} \binom{q}{\nu} \cos\nu\varepsilon \; \frac{(q-2\nu) \; \alpha_1'^{\frac{q}{2}-\nu+\ell} \; (-1)^\ell}{2^q \; \Gamma[q-2\nu+1] \; \gamma_1'^{\ell} \; (\ell!)^2}$$

$$\cdot \; \Gamma[\tfrac{q}{2} - \nu + \ell] \; {}_1F_1[\tfrac{q}{2} - \nu + \ell ; q-2\nu+1 ; -\alpha_1']$$

$$+ \begin{cases} 0, & q : \text{even} \\ \binom{q}{q/2}/2^q, & q : \text{odd} \end{cases} , \qquad (4\text{-}7)$$

where

α_1' : effective up-link carrier-to-noise power ratio (CNR) in (3-6),

γ_{11}' : effective up-link carrier-to-interference power ratio (CIR) in (3-7),

$[q/2]$: greatest integer $< q/2$,

and

$$\binom{q}{\nu} = \frac{q!}{(q-\nu)!\nu!} \quad . \tag{4-8}$$

Next $s_2(q)$ is evaluated in a similar manner of $s_1(q)$ with (4-7).

With the relation of (4-6), (4-5) becomes

$$s_2(q) = \sum_{\nu=0}^{[q/2]} \sum_{\ell=0}^{\infty} \sum_{\eta=0}^{\infty} \varepsilon_{q-2\nu} \binom{q}{\nu} \cos \nu\varepsilon \frac{(-1)^{\ell+\eta}}{2^{2(q+\ell+\eta)-2\nu+1}}$$

$$\cdot \frac{U_0^{\,q-2\nu+2\eta} \left(1+\gamma_0^{-1}+2\gamma_0^{-\frac{1}{2}}\cos\psi_0\right)^{\frac{q-2\nu+2}{2}}}{\eta!(\ell!)^2\,\Gamma[q-2\nu+1]\,\Gamma[q-2\nu+\eta+1]}$$

$$\cdot \frac{I_{11}^{\,2\ell}\,\Gamma[q-2\nu+\eta+\ell+1]}{(\sigma_1/\sqrt{2})^{q-2\nu+2(\ell+\eta)+2}} \int_0^{U_0\Lambda} Z \left(\frac{Z}{\sqrt{2}\sigma_1}\right)^{q-2\nu}$$

$$\cdot \left\{\left(\frac{Z}{U_0(1+\gamma_0^{-1}+2\gamma_0^{-\frac{1}{2}}\cos\psi_0)\,\Lambda}\right)^q - 1\right\}$$

$$\cdot\ {}_1F_1[q-2\nu+\ell+1;q-2\nu+1;\ -Z^2/2\sigma_1^2]\quad dZ\ . \tag{4-9}$$

Expansion of ${}_1F_1[\cdot;\cdot;\cdot]$ with the relations of [42,p.1073]

$${}_1F_1[\alpha;\beta;-x] = \exp(-x)\ {}_1F_1[\beta-\alpha;\beta;x] \tag{4-10}$$

$${}_1F_1[a;c;z] = \frac{\Gamma[c]}{\Gamma[a]} \sum_{n=0}^{\infty} \frac{\Gamma[a+n]\ z^n}{\Gamma[c+n]\ n!} \tag{4-11}$$

yields

$$s_2(q) = \sum_{\nu=0}^{[q/2]} \sum_{\ell=0}^{\infty} \sum_{\eta=0}^{\infty} \sum_{i=0}^{\eta+\ell} \binom{q}{\nu} \varepsilon_{q-2\nu} \cos\nu\varepsilon\ \frac{(-1)^{\ell+\eta}}{2^{q-1}(\eta!)(\ell!)^2(i!)}$$

$$\cdot \frac{\alpha_1'^{\,q-2\nu+\ell+\eta+i+1}\ \Gamma[q-2\nu+\ell+\eta+1]\ \Gamma[i-\eta-\ell]}{\gamma_1'^{\,\ell}\ \Gamma[q-2\nu+\eta+1]\ \Gamma[\ -\eta-\ell]\ \Gamma[i+q-2\nu+1]}$$

$$\cdot \left(\frac{1}{\Lambda^q}\ \beta_{2q-2\nu+2i+1} - \beta_{q-2\nu+2i+1}\ \right)\ , \tag{4-12}$$

where the expression

$$\beta_n = \int_0^{\Lambda\left(1+\gamma_0^{-1}+2\gamma_0^{-\frac{1}{2}}\cos\psi_0\right)^{\frac{1}{2}}} y^n \exp(-\alpha_1' y^2)\ dy \tag{4-13}$$

can be calculated by the recurrence relation :

$$(n+1)\beta_n = \{\Lambda(1+\gamma_0^{-1}+2\gamma_0^{-\frac{1}{2}}\cos\psi_0)^{\frac{1}{2}}\}^{n+1}\exp(-\alpha_1\Lambda^2) + 2\alpha_1'\beta_{n+2} \quad (4\text{-}14)$$

Substituting (4-7), (4-12) into (4-3), the q^{th} moment $m_U(q)$ of the inphase component of $v_2(t)$ is obtained.

(2) Moments of $n_2(t) + i_2(t)$

The characteristic function $M_D(u)$ of the down-link disturbances $n_2(t) + i_2(t)$ is represented by

$$M_D(u) = J_0(I_{21}\,u)\ \exp(-\sigma_2^2\,u^2/2) \quad (4\text{-}15)$$

where I_{21} is the amplitude of the down-link interference, σ_2^2 is the down-link noise power, and $J_0(\cdot)$ is the zero-order Bessel function. The number of down-link interferences is assumed to be one ($a_2=1$). Expansion of $J(\cdot)$ and $\exp(\cdot)$ in (4-15) yields

$$M_D(u) = \sum_{q=0}^{\infty}\ \sum_{h=0}^{q/2} \frac{(-1)^q\ (\sigma_1^2/2)^h\ h\ (I_{21}/2)^{q-2h}}{h!\ (\frac{q-2h}{2}!)^2}\,u^q . \quad (4\text{-}16)$$

Then q^{th} moment $m_D(q)$ of the disturbances $n_2(t) + i_2(t)$ is obtained with the recurrence relations

$$m_D(q) = \begin{cases} \sum_{h=0}^{q/2} m_d(q,h), & q : \text{even} \\ 0, & q : \text{odd} \end{cases} . \quad (4\text{-}17)$$

where

$$\left.\begin{aligned} m_d(q,h) &= m_d(q,h-1)\,\frac{\gamma_{21}\,(\,q/2-h+1\,)^2}{2\alpha_2\,h} \\ m_d(q,h) &= m_d(q-2,h)\,\frac{h\,(q-1)}{2\gamma_{21}\,(q/2-h)^2} \\ m_d(0,0) &= 0 \end{aligned}\right\} \qquad (4\text{-}18)$$

and

α_2 $(=1/2\sigma_2{}^2)$: down-link CNR,

$\gamma_{21}(=1/2I_{21}{}^2)$: down-link CIR.

(3) Probablity Density Function of $u_2(t)$

Since the receiver input wave $u_2(t)$ consists of statistical independent variables $v_2(t)$ and $n_2(t) + i_2(t)$, the p^{th} moment $m_x(p)$ of the inphase component x in Fig.4.1 is represented by

$$m_x(p) = \sum_{q=0}^{p} \binom{p}{q}\, m_U(p-q)\, m_D(q)\,, \qquad (4\text{-}19)$$

where $m_U(q)$ and $m_D(q)$ are given by (4-3) and (4-17) respectively. From (4-19) the conditional p.d.f. $p(x|I_0,\psi_0)$ of x can be derived with the aid of the Gram - Charlier expansion (see APPENDIX C).

$$p(x|I_0,\psi_0) = \sum_{p=0}^{\infty} \frac{F(p)}{p!\sqrt{2\pi}}\quad \exp(-x^2)\, H_p(x)\,, \qquad (4\text{-}20)$$

where

$$F(p) = \sum_{q=0}^{[p/2]} (-1)^q (2q-1)!! \binom{p}{2q} m_x(p-2q) . \qquad (4\text{-}21)$$

and

$$H_p(x) = \sum_{q=0}^{[p/2]} (-1)^q (2q-1)!! \binom{p}{2q} x^{p-2q} \qquad (4\text{-}22)$$

are the Hermite polynomials, also

$$(2i-1)!! = (2i-1)(2i-3)\cdots 3\cdot 1 . \qquad (4\text{-}23)$$

4.3 Error Probability

The error occurs when the inphase component x of the receiver input wave $u_2(t)$ becomes negative under the condition of $\lambda_0=0$. Therefore integrating $p(x|I_0,\psi_0)$ over the error region $x<0$ as shown in Fig.4.1, the conditional error probability $Pes|I_0,\psi_0$ for BPSK becomes

$$Pes|I_0,\psi_0 = \int_{-\infty}^{0} p(x|I_0,\psi_0)\, dx$$

$$= \frac{1}{\sqrt{2\pi}} \int_{-\infty}^{0} \exp(-x^2/2)\, dx - \sum_{p=1}^{\infty} \frac{F(p)}{p!\sqrt{2\pi}} H_{p-1}(0), \qquad (4\text{-}24)$$

where I_0, ψ_0 are the amplitude and the phase of the intersymbol interference component given in (2-13), (2-14). Averaging (4-24) over symbol patterns, the average error probability Pes is

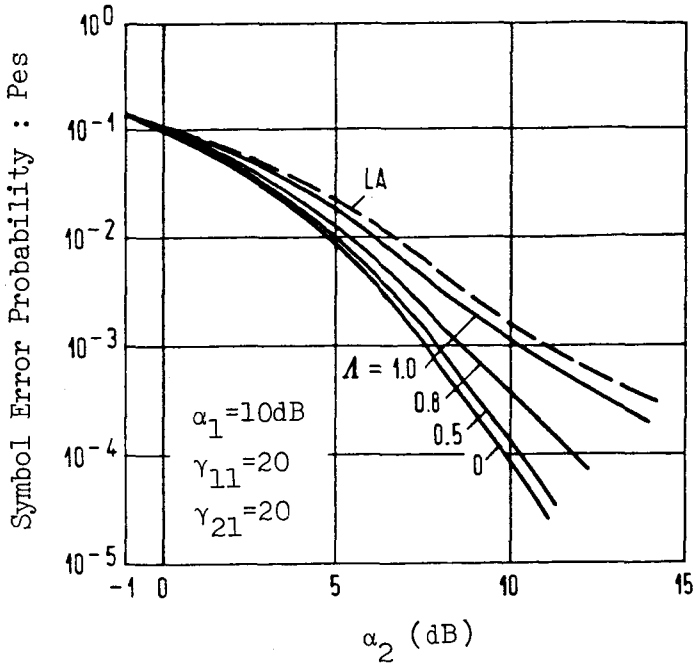

Fig.4.2 Symbol error probability for BPSK
(up-link : one interference + noise
down-link : one interference + noise)

obtained. Including the effects of intersymbol interference due to adjacent symbols, four conditional error probabilities must be calculated in order to get the average error probability, i.e., symbol pattern $\lambda_{-1}, \lambda_0, \lambda_1$: 000, 001, 100, 101 as shown in (3-19)†.

---

† In practical calculations, the moments arround $\langle x \rangle$ is also available to get the coefficient $F(p)$ in (4-21). Then the conditional error probability is expressed by

$$Pes|I_0,\psi_0 = \frac{1}{\sqrt{2\pi}} \int_{-\infty}^{\langle x \rangle} \exp(-x^2/2)\, dx - \sum_{p=1}^{\infty} \frac{F(p)}{p!\sqrt{2\pi}} \exp(-\langle x \rangle^2/2)\, H_{p-1}(\langle x \rangle) .$$

The numerical results of the error probability for no intersymbol interference case are shown by the solid lines in Fig.4.2. To clarify the effects of the soft-limiter, also the error probability for the linear channel is calculated which has linear amplifier (LA) instead of the soft-limiter under the condition that LA output power is 1/2 (refer Section 3.4). The result is shown by broken line in Fig.4.2. In Fig.4.2 the error probability for Λ =0 (hard-limiter) is identical to that of the method in Chapter 3.

First note that the soft-limiting system (Λ=0,$\cdots$,1) is superior to the LA system although the soft-limiter output power is smaller than the LA output power† . The error probability for the soft-limiting system becomes smaller according to decrease ofΛ , and Λ =0 yields the best performance.

Next at Pes=10^{-4} the difference of down-link CNR α_2 between Λ =0 and Λ =0.5 is only 0.5dB. Therefore the region of $\Lambda < 0.5$ (where the limiting-level is lower than half the signal amplitude) is considered to be sufficient for practical uses.

4.4 Concluding Remarks

In this chapter an analytical method has been presented for clarifying the effects of the soft-limiter in BPSK satellite systems in the presence of RF interference. Using the joint p.d.f. of the up-link composite wave the p.d.f. of the received wave has been derived with the aid of the Gram - Charlier expansion. Then by integrating this p.d.f. over the error

---

† Except for Λ =0 : the same output power.

region, the error probability has been obtained. The numerical results have shown that the error probability becomes less according to decrease of the soft-limiter limiting level Λ, and that $\Lambda=0$ yields the best performance. Especially the region of $\Lambda< 0.5$ (where the limiting level is lower than half the signal amplitude) is considered to be suitable for practical uses. The method presented in this chaper is easily extended to the multi-intereference case.

CHAPTER 5

COMPARISON WITH MINIMUM SHIFT KETING SIGNALS

5.1 Introduction

Recently in order to achieve the efficient utilizatin of frequency spectrum, the quadrature carrier modulations with base band pulse shaping or filtering [26],[27] is expected to be more preferable than the phase shift keying (PSK). Especially in the satellite channels, the constant envelope modulations such as quarternary PSK (QPSK)†, offset QPSK (OQPSK), and minimum shift keying (MSK) are considered to be suitable. Murakami, Furua, Matsuo, and Sugiyama have compared the performances of QPSK, OQPSK, and MSK systems in the satellite channels where adjacent channel interferences are taken into accout with both AM-AM, and AM-PM conversions of the satellite travelling wave tube (TWT), and showed that in the narrow-band condition QPSK yielded the best performance, but in the wide-band condition MSK was most preferable [32]. Fang has shown also the superiority of MSK in the wide band condition, and furthermore the hard limiter ahead of the TWT was introduced as an efficient device to improve the performance [33]. These works was performed by computer simulations. In the analytical methods, on the other hand, there are few comparative studies among QPSK, OQPSK, and MSK satellite systems in the presence of radio frequency (RF) interference.

---

† or quadrature PSK

For QPSK, Huang, Omura, and Lindsey have examined the bit error probability with TWT nonlinearlities and RF interference by a two-dimensional moment technique [63]. Especially the hard-limiting channel gives the best performance in any nonlinearities there. But in the analysis method, the expectation with respect to intersymbol interference is a tremendous task because the expectation must be taken for the nonlinear output signal.

In this chapter, the results obtained in Chapter 3 is developed to demonstrate the system comparisons among QPSK, OQPSK and MSK, using an equivalent model in which an intersymbol interference component does not pass through the hard-limiter. That is, in order to avoid the complicated expectation due to the nonlinearity, an equivalent model is newly introduced, where a desired signal is first disturbed by up-link interference and down-link noise before the hard-limiter, then disturbed by the intersymbol interference component, up-link interference, and up-link noise after the hard-limiter. This model has a different amplitude distribution but the same phase distribution at the receiver input as the results of a symmetric property between the both links. The characteristic function of the received inphase channel amplitude is derived using the probability density function (p.d.f.) of down-link phase shift for down-link analysis and the moment technique for up-link analysis. Then the bit error probability is obtained with the aid of the Gram-Charlier expansion in order to compare the system performances among QPSK, OQPSK, and MSK. Furthermore a comparison with the linear channel is made for clarifying the noise margin, the interference margin, or the BT margin due to the hard-limiter [75],[76].

5.2 Minimum Shift Keying Signals

QPSK, OQPSK, and MSK signals are expressed by (see Fig.5.1)

$$u_0(t) = \tilde{u}_0(t) \exp(j 2\pi f_0 t), \tag{5-1}$$

where

$$\tilde{u}_0(t) = \Big[\sum_{m_1} \lambda_{Im_1} \sin\{ g(t+\Delta T - m_1 T) \} \operatorname{rect}\{ (t-m_1 T)/T \} \Big]$$
$$+ j \Big[\sum_{m_2} \lambda_{Qm_2} \sin\{ g(t-m_2 T) \} \operatorname{rect}\{ (t-\Delta T - m_2 T/T \} \Big], \tag{5-2}$$

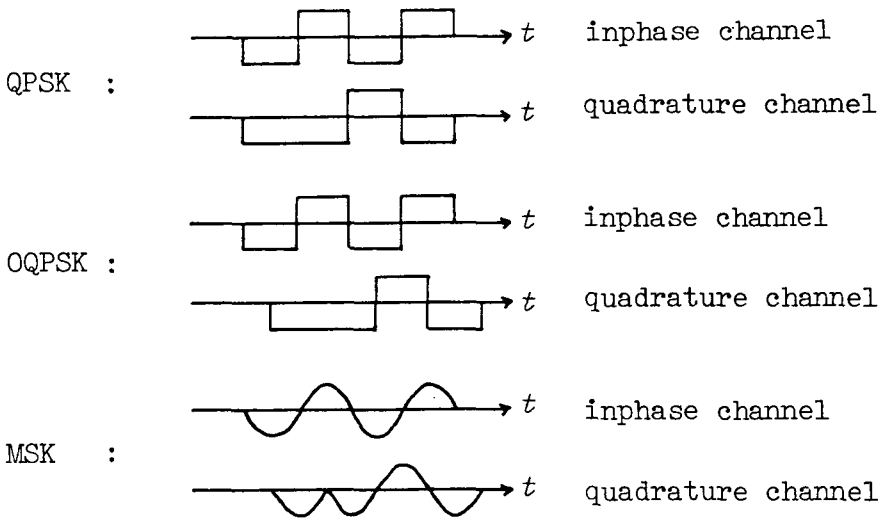

Fig.5.1 Base band pulse shapes of QPSK, OQPSK, and MSK
$\{\lambda_{Im_1}\} = \{0,1,0,1\}$, $\{\lambda_{Qm_2}\} = \{0,0,1,0\}$

$$\Delta = \begin{cases} 1/2, & \text{MSK, OQPSK} \\ 0, & \text{QPSK,} \end{cases} \tag{5-3}$$

$$g(t) = \begin{cases} \pi t/T & \text{MSK} \\ \pi/4, & \text{QPSK, OQPSK,} \end{cases} \tag{5-4}$$

and f_0 is the carrier frequency, T is the symbol duration, λ_{Im_1} and λ_{Qm_2} (± 1) are binary messages of inphase and quadruture channels respectively, and rect($\cdot$) is the window function defined in (2-3). After passing through the transmit filter,

$$v_1(t) = \tilde{v}_1(t) \exp(j 2\pi f_0 t), \tag{5-5}$$

where

$$\tilde{v}_1(t) = \left[\sum_{m_1} \lambda_{Im_1} q(t - m_1 T) \right] + j \left[\sum_{m_2} \lambda_{Qm_2} q(t - \Delta T - m_2 T) \right]. \tag{5-6}$$

In (5-6), $q(t)$ is the single pulse responce for QPSK, OQPSK, or MSK, and defined by

$$q(t) = \begin{cases} \int_{-\infty}^{\infty} \text{rect}\{\tau/T\}\, \tilde{h}(t-\tau)\, d\tau, & \text{QPSK, OQPSK} \\ \int_{-\infty}^{\infty} \text{rect}\{\tau/T\}\, \sin\{\pi(\tau + T/2)/T\}\, \tilde{h}(t-\tau)\, d\tau, & \text{MSK,} \end{cases} \tag{5-7}$$

where $\tilde{h}(t)$ is the lowpass equivalent impulse response of the transmit filter, and $f_0 T$ is an integer. Since it is assumed that the inphase and quadruture channels are symmetric, and λ_{Im_1} and λ_{Qm_2} are equiprobable, only the analysis in the inphase channel is represented without loss of generality. (5-6) is rewritten as

$$\tilde{v_1}(t) = \tilde{u_0}(t) + \tilde{i_0}(t) \tag{5-8}$$

where

$$\tilde{u_0}(t) = q(t) \exp(j2\pi f_0 t) \tag{5-9}$$

$$\tilde{i}_0(t) = \{ i_{0C}(t) + j\, i_{0S}(t) \} \exp(j2\pi f_0 t), \tag{5-10}$$

and

$$i_{0C}(t) = \sum_{\substack{m_1 \\ (m_1 \neq 0)}} \lambda_{Im_1} q(t - m_1 T), \tag{5-11}$$

$$i_{0S}(t) = \sum_{m_2} \lambda_{Qm_2} q(t - \Delta T - m_2 T). \tag{5-12}$$

Note that $\tilde{u_0}(t)$ is the desired signal in the inphase channel, and $\tilde{i_0}(t)$ are an intersymbol interference component due to both the inphase and the quadruture channels. In Fig.5.2(a), the transmit filter ouput $v_1(t)$ is transmitted through the band pass hard-limiter (BPHL) with the disturbances of RF interference $i_1(t)$, $i_2(t)$ and Gaussian noise $n_1(t)$, $n_2(t)$ on both up-link and

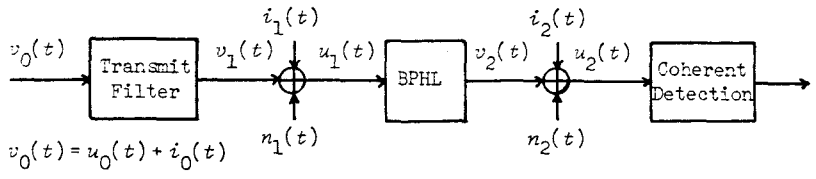

(a) Conventional model

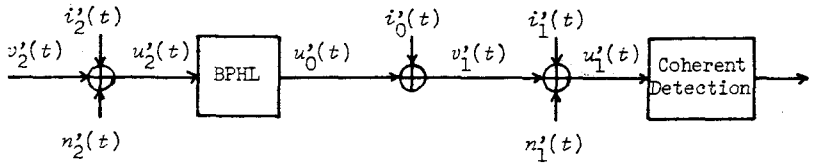

(b) Equivalent model

Fig.5.2 Model for hard-limiting satellite system

down-link in (2-20)-(2-22). The output of the BPHL has a constant envelope and the same phase angle as that of the input [41].

5.3 Equivalent Model for Error Probability Analysis

In this section, an equivalent model for the error probablity analysis is introduced. For zero phase transmitted (λ_{IO} =0), an error occurs when the inphase component x of the received wave becomes negative in Fig.5.3(a). This event corresponds to the event that $\pi/2 < \phi_2 < 3\pi/2$. Therefore the bit error probability Peb becomes

$$\begin{aligned} \text{Peb} &= \text{probablity}\ [x < 0] \\ &= \text{probablity}\ [\pi/2 < \phi_2 < 3\pi/2]. \end{aligned} \tag{5-13}$$

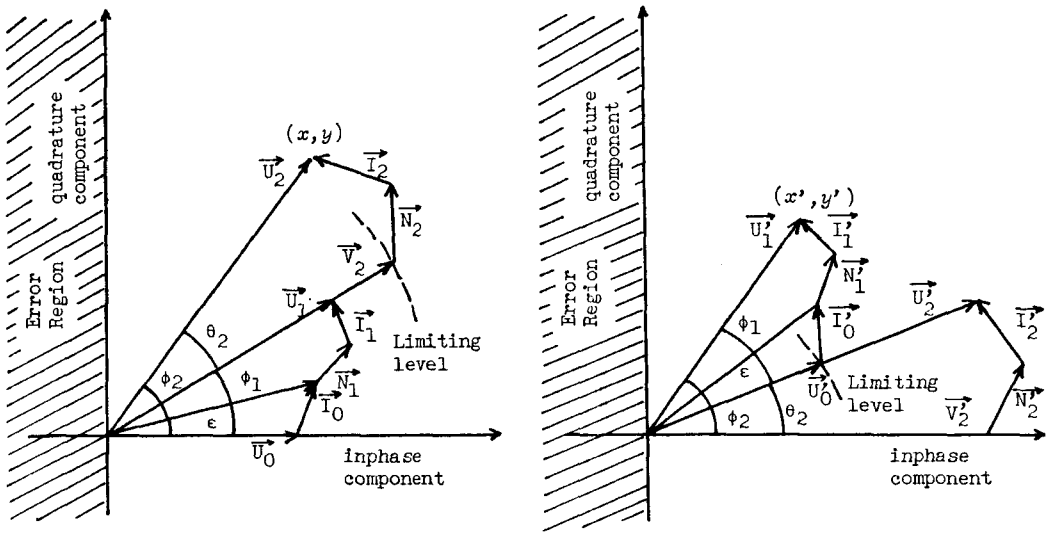

(a) Vector diagram and error region in conventional model.

(b) Vector diagram and error region in euivalent model.

Fig.5.3 Vector diagram and error region in hard-limiting satellite system.

Hence, if an equivalent system in Fig.5.2(b) has the same statistical properties of ϕ_2 , the both systems of Fig.5.2(a) and Fig.5.2(b) yield the same error probability.

The received phase ϕ_2 in Fig.5.3(a) consists of the up-link phase shift ϕ_1 and the down-link phase shift θ_2 as

$$\phi_2 = \phi_1 + \theta_2 \quad . \tag{5-14}$$

Here, the up-link phase shift ϕ_1 depends only on the up-link parameters : up-link carrier-to-noise power ratio (CNR) α_1 , up-link carrier-to-interference power ratio (CIR) γ_{1n} $(n=1,\cdots,a_1)$, and carrier-to-intersymbol interference power ratio γ_0 as shown in (3-12). On the other hand the down-link

phase shift θ_2 depends only on the down-link parameters : down-link CNR α_2 , down-link CIR γ_{2i} (i=1,$\cdots$,a_2) as shown in (3-13). Therefore due to the statistical independence of both the up-link and the down-link, an exchange of the up-link and the down-link is possible to get the same statistical properties of the received phase. That is, in the euivalent model in Fig.5.2(b) and Fig.5.3(b), the desired signal is disturbed by the down-link interference and noise before entering the BPHL, and disturbed by the intersymbol interference component, up-link inteference, and up-link noise after passing through the BPHL. Though the amplitude distribution of $u_1'(t)$ in Fig.5.2(b) is different from that of $u_2(t)$ in Fig.5.2(a), the received phase of both $u_1'(t)$ and $u_2(t)$ have the same distribution. Therefore the error probability can also represented by

$$\text{Peb} = \text{Probability}\ [\ x' < 0\ ]\ . \tag{5-14}$$

Here note that the BPHL output power can be chosen arbitrary, so long as the parameters of CNR's and CIR's are fixed.

5.4 Probability Density Function in Equivalent Model

In this section the p.d.f. of the inphase component x' in Fig.5.3(b) is derived. In Fig.5.2(b) and Fig.5.3(b), the receiver input $u_1'(t)$ is represented by

$$u_1'(t) = u_0'(t) + i_0'(t) + i_1'(t) + n_1'(t), \tag{5-15}$$

where

$$u_0'(t) = q(0)\exp[j\{2\pi f_0 t + \theta_2(t)\}], \tag{5-16}$$

$$i_0'(t) = i_0(t)\exp\{j\theta_2(t)\}, \tag{5-17}$$

$$i_1'(t) = i_1(t)\exp\{j\theta_2(t)\}, \tag{5-18}$$

$$n_1'(t) = n_1(t)\exp\{j\theta_2(t)\}, \tag{5-19}$$

and $\theta_2(t)$ is the phase difference between $v_2'(t)$ and $u_2'(t)$. Here, since the BPHL output level can be chosen arbitrary so long as the CNR's and CIR's are fixed, the BPHL output level is set to $q(0)$ for convenience. That is, it is assumed that the desired signal power at the transmitter output equals to the BPHL power. The characteristic function $M_{x'}(u)$ of x' is derived at the sample instant t_0 which is a midpoint of the symbol. From now on, the subscript t_0 is omitted for simplicity. Using (5-11), (5-12), (5-15)-(5-19), the inphase component x' in Fig.5.3(b) is expressed by

$$x' = (i_{0C}+1)\cos\theta_2 - i_{0S}\sin\theta_2 + w, \tag{5-20}$$

where

$$w = \sum_{n=1}^{a_1} I_{1n}\cos(\psi_{1n}+\theta_2) + \tilde{n_1}\cos(\zeta_1+\theta_2). \tag{5-21}$$

Also i_{OC}, i_{OS} are the inphase and the quadrature components of intersymbol interference given in (5-11),(5-12), and w is due to the up-link interferences and noise in (2-20)-(2-22). The characteristic function $M_{x'}(u)$ is defined by

$$M_{x'}(u) = < \exp(jux') >$$

$$= \sum_{p=0}^{\infty} m_{x'}(p) (ju)^p / p! \ , \qquad (5\text{-}22)$$

where $<\cdot>$ denotes the expectation, and $m_{x'}(p)$ is a p^{th} moment of x'. Using (5-20), $m_{x'}(p)$ is expressed by

$$m_{x'}(p) = \sum_{b=0}^{p} \sum_{c=0}^{b} \sum_{d=0}^{c} \binom{p}{b} \binom{b}{c} \binom{c}{d} (ju)^p / p!$$

$$\cdot < i_{OC}{}^{d} \, i_{OS}{}^{b-c} \cos^{c}\theta_2 \sin^{b-c}\theta_2 \, w^{p-b} > \ , \qquad (5\text{-}23)$$

where $\binom{p}{b}$ is the combination in (4-8). Now in (5-21), Since, the phases ψ_{1n} of the up-link n^{th} interference $i_{1n}(t)$ and ζ_1 of the up-link noise $n_1(t)$ are uniformly distributed on $(0,2\pi)$, then $\psi_{1n}+\theta_2$ and $\zeta_1+\theta_2$ are also uniformly distributed independently of θ_2. Then the expectation in (5-23) can be devided into three parts, using the statistical independence among i_{OC}, i_{OS}, θ_2, and w. Furthermore since i_{OC}, i_{OS} have symmetrical distributions,

$$< i_{OC}{}^{d} \, i_{OS}{}^{b-c} > = 0, \qquad d, \ b-c : \text{odd} \ . \qquad (5\text{-}24)$$

Therefore (5-23) can be rewritten as

$$m_{x'}(p) = \sum_{b=0}^{p} \sum_{c=0}^{b} \sum_{d=0}^{c} \sum_{e=0}^{(b-c)/2} \binom{p}{b} \binom{b}{c} \binom{c}{d} \binom{\frac{b-c}{2}}{e} (-1)^e \cdot (ju)^p / p!\; q(0)^{c-d}\; m_{\theta_2}(c+2e)\; m_{I_0}(d, b-c)\; m_w(p-b), \quad (b-c, d: \text{even})$$

(5-25)

where

$$m_{\theta_2}(q) = \langle \cos^q \theta_2 \rangle, \quad (5\text{-}26)$$

$$m_{I_0}(r_1, r_2) = \langle i_{0C}^{\,r_1}\, i_{0S}^{\,r_2} \rangle, \quad (5\text{-}27)$$

$$m_{U'}(q) = \left\langle \left\{ \sum_{n=1}^{a_1} I_{1n} \cos(\psi_{1n}) + \tilde{n}_k \cos(\zeta_k) \right\}^q \right\rangle. \quad (5\text{-}28)$$

(1) Derivation of $m_{\theta_2}(q)$

The p.d.f. $p(\theta_2)$ is derived as $p(\phi_2 | \phi_1)$ in (3-13) where $\theta_2 = \phi_2 - \phi_1$. Therefore using the relation of (4-6), $m_{\theta_2}(q)$ is obtained as

$$m_{\theta_2}(q) = \int_{-\infty}^{\infty} \cos^q \theta_2 \; p(\theta_2)\, d\theta_2$$

$$= \sum_{\substack{\nu=0 \\ 2\nu \neq q}}^{[\frac{q}{2}]} \frac{(q-2\nu)\ \binom{q}{\nu}}{2^q\, \Gamma(q-2\nu+1)} f_2(q-2\nu) + \begin{cases} 0 & q: \text{odd} \\ 2^{-q} \binom{q}{q/2}, & q: \text{even} \end{cases}, \quad (5\text{-}29)$$

where

$f_2(\nu)$=(3-13b).

(2) Derivation of $m_{I_0}(r_1, r_2)$

The joint moment $m_{I_0}(u,v)$ can be derived from the characteristic function of intersymbol interference. For convenience, $R_I(m_1)$ and $R_Q(m_2)$ are defined as

$$R_I(m_1) = q(m_1 T),\ m_1=\pm1,\pm2,\cdots,\pm L_I \ : \text{QPSK,OQPSK,MSK} \tag{5-30}$$

$$R_Q(m_2) = \begin{cases} q(m_2 T),\ m_2=0,\pm1,\pm2,\cdots,\pm L_I \ : \text{QPSK} \\ q(m_2 T+\Delta T),\ m_2=-L_I,\cdots,-1,0,1,\cdots,L_I-1 \\ \qquad\qquad : \text{OQPSK,MSK} \end{cases} \tag{5-31}$$

where $q(t)$ is the pulse responce of the transmit filter in (5-7), m_1 and m_2 are the symbol numbers in both inphase and quadrature channels. In what follows, the effects of intersymbol interference due to previous L_I and consective L_I symbols are icluded for each channel. Using (5-30), (5-31), the characteristic function $M_{I_0}(u,v)$ is

$$\begin{aligned} M_{I_0}(u,v) &= \left\langle \prod_{m_1,m_2} \exp\{juR_I(m_1) + jvR_Q(m_2)\} \right\rangle \\ &= \prod_{m_1} \cos\{R_I(m_1)u\} \cdot \prod_{m_1} \cos\{R_I(m_2)v\}. \end{aligned} \tag{5-32}$$

To evaluate (5-32), first expanding $\cos[R_I(m_1)]$ with the g^{th} cumulant $B_I^{(m_1)}(g)$ of $R_I(m_1)$,

$$\cos\left[R_I(m_1)u\right] = \exp\left\{\sum_{g=0}^{\infty} B_I^{(m_1)}(g)\,\frac{(ju)^g}{g!}\right\}, \tag{5-33}$$

where $B_I^{(m_1)}(g)$ is derived by recurrence relations [63] :

$$B_I^{(m_1)}(g) = A(2g)(-1)^g(2g)!R_I^{2g}(m_1), \tag{5-34}$$

and

$$\left.\begin{aligned} A(2g) &= \frac{(-1)}{(2g)!} - \sum_{k=1}^{g-1}(-1)^{g-k}\,\frac{k}{g}\,\frac{A(2g)}{\{2(g-k)\}!} \\ A(2g+1) &= 0 \\ A(2) &= -1/2 \end{aligned}\right\}, \tag{5-35}$$

which are given from the derivative of (5-33). From the statistical independence among symbol series,

$$\prod_{m_1}\cos\{R_I(m_1)u\} = \exp\left\{\sum_{g=0}^{\infty} B_I(g)(ju)^g/g!\right\}, \tag{5-36}$$

where

$$B_I(g) = \sum_{m_1} B_I^{(m_1)}(g). \tag{5-37}$$

Expanding exp(·) in (5-36),

$$\prod_{m_1} \cos\{R_I(m_1)u\} = \sum_{g=0}^{\infty} D_I(g)(ju)^g/g!\,, \tag{5-38}$$

where

$$\left.\begin{aligned} D_I(g) &= \sum_{i=1}^{g} \binom{g-1}{i-1} B_I(i)\ D_I(g-i) \\ D_I(0) &= 1 \end{aligned}\right\}, \tag{5-39}$$

Next the components of $R_Q(m_2)$ can be rewritten in a similar fashion as that of $R_I(m_1)$.

$$\prod_{m_2} \cos\{R_Q(m_2)v\} = \sum_{h=0}^{\infty} D_Q(h)(jv)^h/h!\,, \tag{5-40}$$

where

$$\left.\begin{aligned} D_Q(h) &= \sum_{i=1}^{h} \binom{h-1}{i-1} B_Q(i)\ D_Q(h-i) \\ D_Q(0) &= 1 \end{aligned}\right\}, \tag{5-41}$$

$$B_Q(h) = \sum_{m_2} B_Q^{(m_2)}(h), \tag{5-42}$$

and

$$B_Q^{(m_2)}(h) = A(2h)(-1)^h(2h)!R_Q^{2h}(m_2). \tag{5-43}$$

Thus from (5-38) and (5-40), the characteristic function $M_{I_O}(u,v)$

becomes

$$M_{I_0}(u,v) = \sum_{r_1=0}^{} \sum_{r_2=0}^{} m_{I_0}(r_1, r_2) \frac{(ju)^{r_1}(jv)^{r_2}}{r_1!\ r_2!}, \quad (5\text{-}44)$$

where

$$m_{I_0}(r_1, r_2) = \sum_{g=0}^{\infty} \sum_{h=0}^{\infty} D_I(g) D_Q(h) \frac{(ju)^g (jv)^h}{g!\ h!}. \quad (5\text{-}45)$$

(3) Derivation of $m_U,(q)$

w is composed of the up-link interference $i_1(t)$ and the up-link noise $n_1(t)$. The moments of w are obtained in a similar manner in Section 4.2 (b). In the case of one interference in the up-link ($a_1=1$), the q^{th} moment of w becomes

$$m_U,(q) = \begin{cases} \sum_{h=0}^{q/2} m_u,(q,h), & q : \text{even} \\ 0, & q : \text{odd} \end{cases}, \quad (5\text{-}46)$$

where

$$\left.\begin{aligned} m_u,(q,h) &= m_u,(q,h-1) \frac{\gamma_{11}\left(\frac{q}{2}-h+1\right)^2}{2\alpha_1 h} \\ m_u,(q,h) &= m_u,(q-2,h) \frac{h(q-1)\, q(0)^2}{2\gamma_{11}\left(\frac{q}{2}-h\right)^2} \\ m_u,(0,0) &= 1 \end{aligned}\right\}. \quad (5\text{-}47)$$

and

α_1 ($=q(0)^2/2\sigma^2$) : up-link CNR,

γ_{11} ($=q(0)^2/I_{11}^2$) : up-link CIR.

Therefore from (5-22),(5-25),(5-29),(5-45),(5-46), the characteristic function $M_{x'}(u)$ is obtained.

Using the $M_{x'}(u)$, the p.d.f. $p(x')$ is represented by

$$p(x') = \int_{-\infty}^{\infty} M_{x'}(u) \exp(-jux')\, dx'$$

$$= \int_{-\infty}^{\infty} \sum_{p=0}^{\infty} \frac{(ju)^p}{p!} m_{x'}(p) \exp(-jux)\, dx' \qquad (5\text{-}48)$$

This integration can be performed with the aid of the Gram-Charlier expansion as (see APPENDIX C)

$$p(x') = \sum_{p=0}^{\infty} \frac{F'(p)}{p!\sqrt{2\pi}} \exp(-x'^2/2)\, H_p(x). \qquad (5\text{-}50)$$

where

$$F'(p) = \sum_{q=0}^{[p/2]} (-1)^q (2q-1)!! \binom{q}{2q} m_{x'}(p-2q) \qquad (5\text{-}51)$$

Also $(2q-1)!!$ = (4-23), and $H_p(\cdot)$ are the Hermite polynomials in (4-22).

5.5 Error Probability

In the inphase channel with $\lambda_{I_0}=0$, the error occurs when x' becomes negative. Therefore the bit error probability Peb is obtained by integrating $p(x')$ over the error region $(0, -\infty)$,

$$\text{Peb} = \int_{-\infty}^{0} p(x')\, dx'$$

$$= \frac{1}{\sqrt{2\pi}} \int_{-\infty}^{0} \exp(-x^2/2)\, dx - \sum_{p=1}^{\infty} \frac{F'(p)}{p!\sqrt{2\pi}} H_{p-1}(0). \tag{5-32}$$

In numerical calculations, the cosine roll off filter in (2-16) is utilized for the transmit filter. For the cosine roll off filter, the pulse responce $q(t)$ of the transmit filter for QPSK, OQPSK, and MSK are derived in forms involving sine and cosine integrals (see APPENDIX A). The numerical results of the bit error probability Peb of the hard-limiting (HL) system are shown by the solid lines in Figs.5.4-5.11, where $L_I=5$ is used for the effects of intersymbol interference. To clarify the effects of the hard-limiter, also the bit error probabilities in the linear channel are shown by the broken lines in Figs.5.6-5.9. In the linear channel analysis, a linear amplifier (LA) is used instead of the BPHL in Fig.5.2(a) (cf. Section 3.4).

In Figs.5.4-5.11, η_R is a roll off factor, and B is a 6dB band width of the transmit filter. First, the band limiting effects between QPSK, OQPSK, and MSK are compared in the hard-limiting channel. Fig.5.4 shows the superiority of MSK in the

---

cf. foot note on page 49.

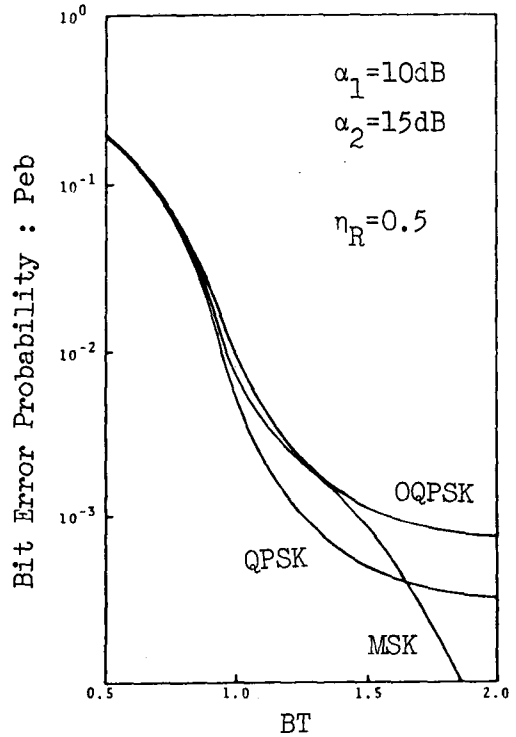

Fig.5.4 Bit Error Probability for QPSK, OQPSK, and MSK
(up-link : noise only,
down-link : noise only)

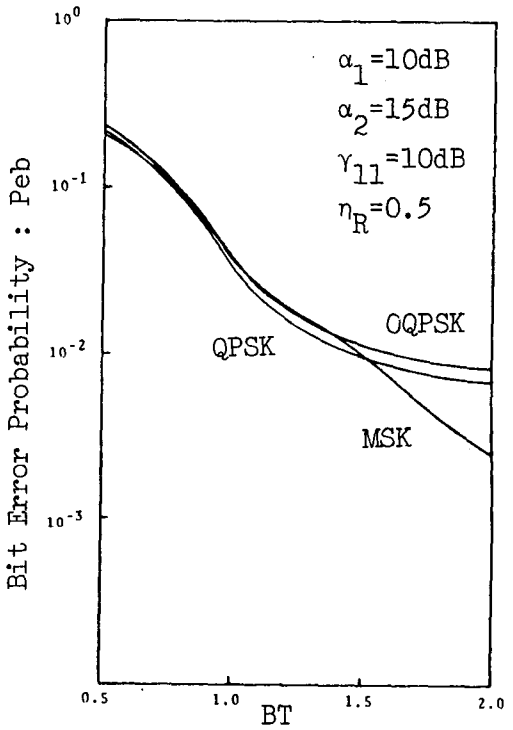

Fig.5.5 Bit Error Probability for QPSK, OQPSK, and MSK
(up-link : one interference + noise, down-link : noise only)

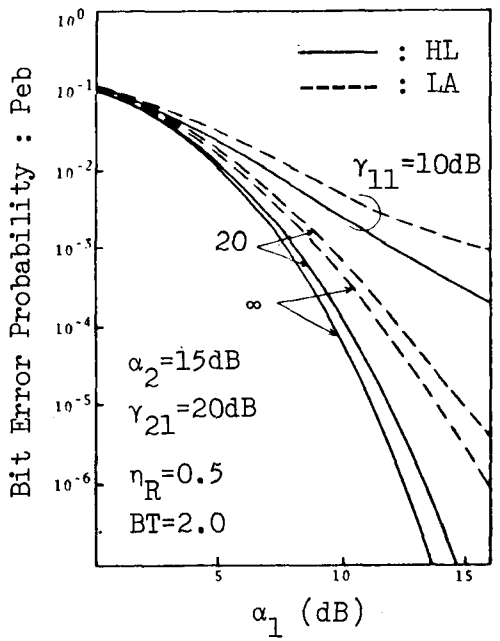

Fig.5.6 Bit Error Probability for MSK (up-link, down-link : one interference + noise)

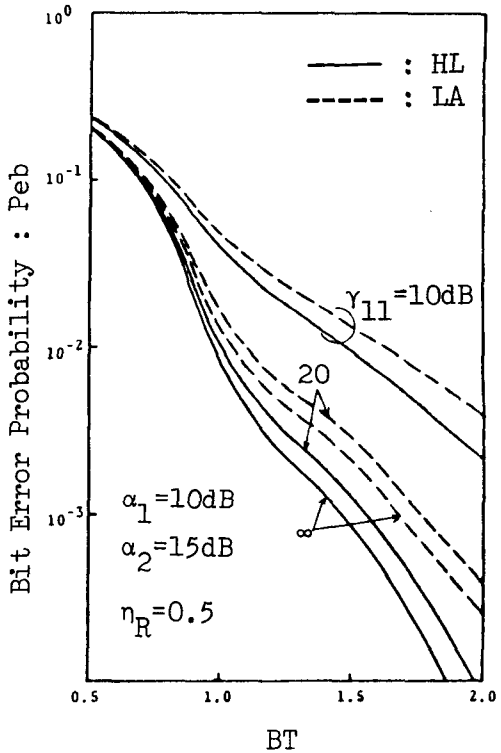

Fig.5.7 Bit Error Probability for MSK (up-link : one interference + noise, down-link : noise only)

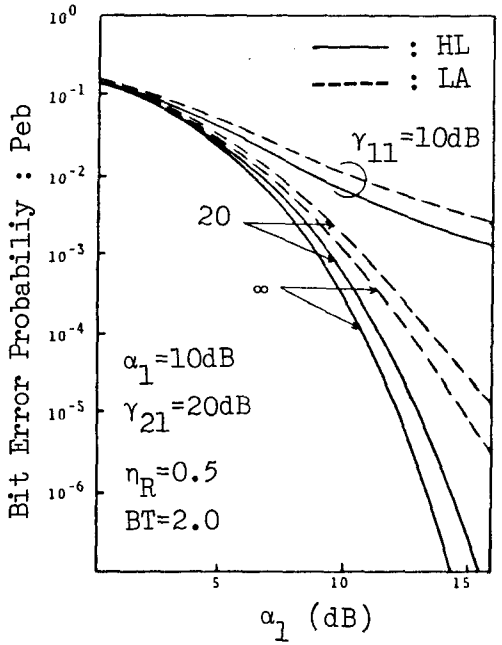

Fig.5.8 Bit Error Probability for QPSK (up-link, down-link : one interference + noise)

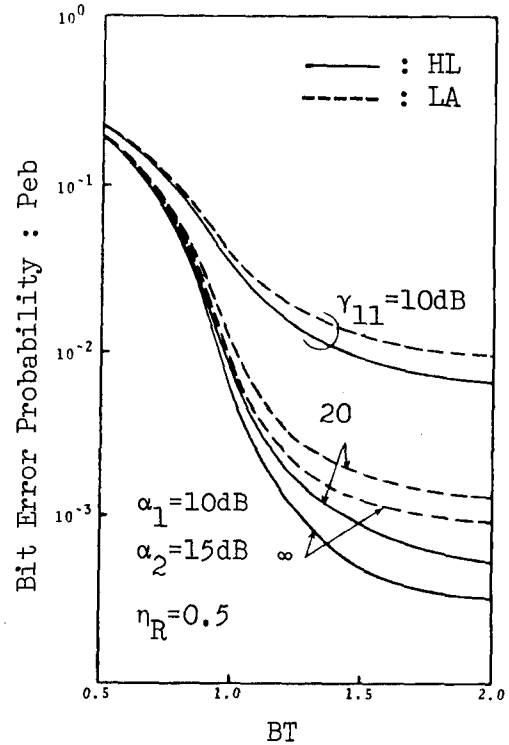

Fig.5.9 Bit Error Probability for QPSK (up-link : one interference + noise, down-link : noise only)

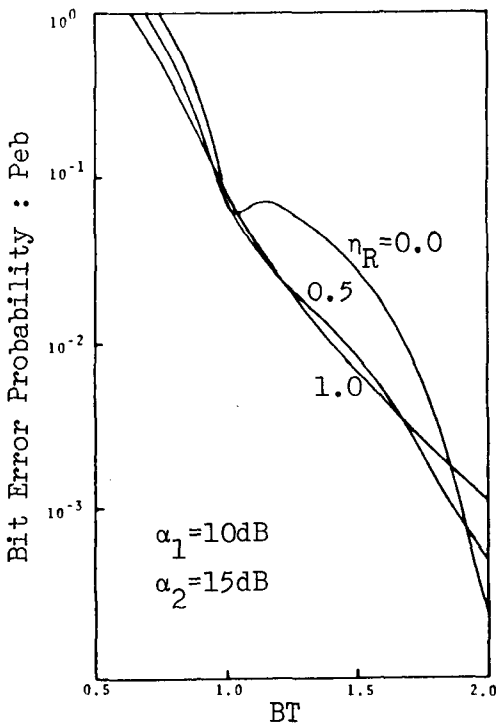

Fig.5.10 Bit Error Probability for MSK
(up-link : noise only,
down-link : noise only)

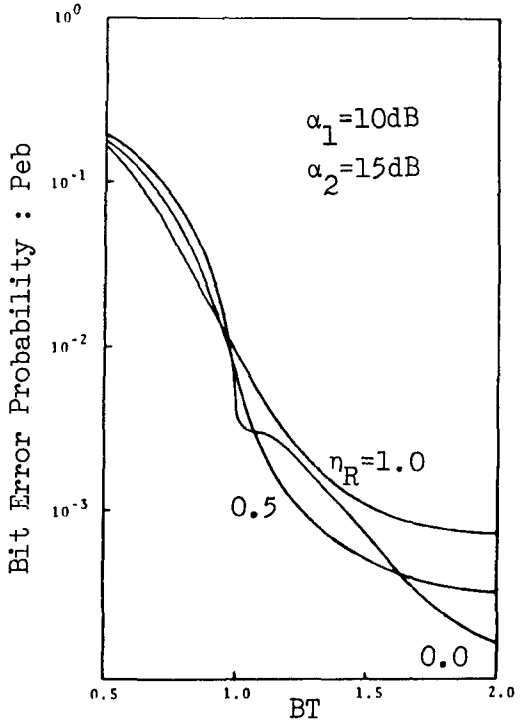

Fig.5.11 Bit Error Probability for QPSK
(up-link : noise only,
down-link : noise only)

region of BT>1.65, but in the smaller BT region QPSK outperforms MSK, which was observed by the earlier computer simulations [32],[33]. Note further that in no interference case of Fig.5.4, the crossing of the error probability curves between QPSK and MSK occurs at BT=1.65, but in the presence of up-link interference (CIR : γ_{11} =10dB) of Fig.5.5, the crossing occurs at less BT (=1.50). The physical understanding of this phenomenon can be made by using a simplified model without intersymbol interference. In the sampling instant, for MSK, an instanteneous power of the desired signal in the inphase channel equals to the total signal power because the power of the quadrature channel is zero for MSK (see Fig.5.1). On the other hand, for QPSK, the power of the desired signal in the inphase chnnel is half of the total signal power. Thus in the condition that both MSK and QPSK have the same total signal power, the effective signal power of MSK is 3dB larger than that of QPSK. In this analysis, CIR is defined as the total signal power - to - interference power ratio. Therefore the effective CIR of MSK is 3dB larger than that of QPSK. This CIR margin of MSK which may decrease with the intersymbol interference is considered to affect the error probability significantly. In the presence of a strong interference, MSK may be more preferable than QPSK even if the BT becomes smaller.

Second, the error probability improvements due to the hard-limiter are compared between MSK and QPSK. In Figs.5.6-5.9, the HL system yields the better performance than the LA system in almost all practical values of the parameters. From Fig.5.6 for MSK, it is found that the HL system has the α_1 (up-link CNR) margin of 3dB at ($Pe=10^{-3}$,γ_{11}=20dB) compared with the LA system. Furthermore the error probability for the HL system at γ_{11} =20dB

is better than that for the LA sytem at $\gamma_{11} = \infty$. Therefore the HL system has the γ_{11} (up-link CIR) margin of more than 20dB in this region. Fig.5.7 shows that HL system has the superiority of the BT margin of 0.2 at ($Pe=10^{-3}, \gamma_{11} = 20dB$). For QPSK in Figs.5.8-5.9, it is also observed that the error probability improvements due to the hard-limiter as well as in MSK case, but the error probability is worse than that of MSK in both the HL and the LA systems because of the large BT (=2.0).

Next the effects of the roll off factor η_R on the bit error probability are examined for QPSK and MSK. In Fig.5.10 for MSK, in the region of small BT (< 1.0) the curve for $\eta_R = 1.0$ gives the best performance in the three cueves, but in the region of large BT (> 1.9) the curve for $\eta_R = 0.0$ is more preferable. The error probability is a monotonic function of BT, except for $\eta_R = 0.0$, where the intersymbol interference component with the complicated zero crossing of $q(t)$ makes the curve unpredictable. These effects also exist in QPSK case of Fig.5.11.

5.6 Concluding Remarks

In this chapter, the analytical method has been presented for demonstrating the effects of band-limiting on QPSK, OQPSK and MSK in the hard-limiting satellite systems with RF interference. The equivalent system model has been introduced in which the intersymbol interference component does not pass through the hard-limiter. Using this model, the characteristic function of the received amplitude in the inphase channel has been derived without the complicated expectation with respect to the intersymbol interference component at the nonlinear output. Then

the bit error probability has been obtained with the aid of the Gram-Charlier expansion.

The numerical results have shown that in the region of small BT QPSK was better than MSK or OQPSK, but the smaller BT or the existence of interference made MSK preferable compared with QPSK or OQPSK. Furthermore the comparison with the linear channel has been made for clarifying the effects of the hard-limiter, and the CNR margin, the CIR margin, or the BT margin of the hard-limiter has been discussed. The method presented here is applicapable to any non-Gaussian up-link interferers whose moments are known. But another problems of nonlinear output spectrum, another type nonlineality and optimum pulse shaping have been remained for further investigations.

CHAPTER 6

CONCLUSIONS

This work has analytically investigated the error performances of phase shift keying (PSK) signals in nonlinear channels. As typical nonlinear channels, the satellite channels have been introduced : the band-limited M-ary PSK signal is transmitted through the hard-limiting or soft-limiting satellite transponder with the disturbances of radio frequency (RF) interferences and Gaussian noises in both up-link and down-link. The probability density functions of the received waves have been utilized to obtain the error probabilities. The obtained expressions for the error probabilities are analytically tractable and applicable to arbitrary numbers of modulating phases, nonlinearities, interferences and repeaters. The error probabilty improvements due to the limiter have been discussed through a comparison with the linear channel. Furthermore, in order to clarify the error performance of PSK in the nonlinear channels, a comparison with the minimum shift keying (MSK) system has been performed, introducing a new equivalent model.

The main results obtained in this work can be summarized as follows.

(1) The satellite system equiped with the hard-limiter on board yields the remarkable error probability improvement due to the noise suppression, the interference suppression and the intersymbol interference suppression effects of the hard-limiter. Especially the hard-limiter suppresses

interferences more strongly than noise. In the case where the transmission system is composed of multi-hard-limiting repeater, the increase of the number of repeaters does not severely degrade the error probability compared with the linear channel case.

(2) The error probability of the soft-limiting system becomes smaller according to the decrease of the soft-limiter limiting level, and the hard-limiter case yields the lowest error probability. The limiting level of half the signal amplitude is considered to be sufficient to get the fairly good performance.

(3) In the hard-limiting channel, the error performance of PSK is better than that of MSK in the narrow-band condition. But in the wide-band condition or in the presence of strong interferences, MSK becomes more preferable than PSK.

APPENDIX A

Base-Band Pulse Wave Forms

(1) Rectangular Pulse Responce of the Transmit Filter

The rectangular pulse responce of the transmit filter is expressed by

$$q(t) = \int_{-\infty}^{\infty} \tilde{H}(f)\ \tilde{V_0}(f)\ \exp(j2\pi ft)\ df\ , \qquad \text{(A-1)}$$

where $\tilde{H}(f)$ is the cosine roll off filter transfer function in (2-16), and $\tilde{V_0}(f)$ is

$$V_0(f) = \int_{-T/2}^{T/2} \mathrm{rect}\{\frac{t}{T}\}\ \exp(-j2\pi ft)\,dt = \frac{\sin\pi fT}{\pi f}\ . \qquad \text{(A-2)}$$

Then, using (A-1),(A-2) and (2-16), $q(t)$ becomes

```
q(t) =   1/Pi   [ Sl(B(1-E)/2,Pi(T+2t)) - Sl(B(1-E)/2,Pi(T-2t)) ]†
       + 1/Pi/2 [ Sl(B(1+E)/2,Pi(T+2t)) - Sl(B(1-E)/2,Pi(T+2t)) ]
       + 1/Pi/2 [ Sl(B(1+E)/2,Pi(T-2t)) - Sl(B(1-E)/2,Pi(T-2t)) ]
       + cos(Pi/2/E)/4 [  Cl(B(1+E)/2,Pi(T+2t+1/E/B))
                        - Cl(B(1-E)/2,Pi(T+2t+1/E/B)) ]
       + sin(Pi/2/E)/4 [  Sl(B(1+E)/2,Pi(T+2t+1/E/B))
                        - Sl(B(1-E)/2,Pi(T+2t+1/E/B)) ]
       + cos(Pi/2/E)/4 [  Sl(B(1+E)/2,Pi(T-2t+1/E/B))
                        - Sl(B(1-E)/2,Pi(T-2t+1/E/B)) ]
```

$$
\begin{aligned}
&+ \sin(Pi/2/E)/4\ [\ \ Si(B(1+E)/2,Pi(T-2t+1/E/B)) \\
&\qquad\qquad - Si(B(1-E)/2,Pi(T-2t+1/E/B))\ ] \\
&- \cos(Pi/2/E)/4\ [\ \ Si(B(1+E)/2,Pi(T+2t-1/E/B)) \\
&\qquad\qquad - Si(B(1-E)/2,Pi(T+2t-1/E/B))\ ] \\
&+ \sin(Pi/2/E)/4\ [\ \ Si(B(1+E)/2,Pi(T+2t-1/E/B)) \\
&\qquad\qquad - Si(B(1-E)/2,Pi(T+2t-1/E/B))\ ] \\
&- \cos(Pi/2/E)/4\ [\ \ Si(B(1+E)/2,Pi(T-2t-1/E/B)) \\
&\qquad\qquad - Si(B(1-E)/2,Pi(T-2t-1/E/B))\ ] \\
&+ \sin(Pi/2/E)/4\ [\ \ Si(B(1+E)/2,Pi(T-2t-1/E/B)) \\
&\qquad\qquad - Si(B(1-E)/2,Pi(T-2t-1/E/B))\ ],\ E\neq 0
\end{aligned}
\qquad \text{(A-3)}
$$

where

B : 6dB bandwidth of the transmit filter,

T : symbol duration,

$E=\eta_R$: roll off factor of the transmit filter,

$Pi=\pi$,

and

$$
Si(x,y) = \int_0^{xy} \frac{\sin z}{z}\, dz \qquad \text{(A-4)}
$$

$$
Ci(x,y) = \begin{cases} -\int_{xy}^{\infty} \frac{\cos z}{z}\, dz, & y\neq 0 \\ ln(|x|), & y=0,\ x\neq 0 \\ 0, & y=0,\ x=0 \end{cases} \qquad \text{(A-5)}
$$

Here, the time delay t_0 of the transmit filter is assumed to be zero, and the terms with † are utilized for $\eta_R=0$ (E=0).

(2) Half-Sin Pulse Responce of the Transmit Filter

Fot the half-sin pulse, $\tilde{V}_0(f)$ is represented by

$$\tilde{V}_0(f) = \int_{-T/2}^{T/2} \sin \frac{\pi(t+T/2)}{T} \exp(-j2\pi ft)\, df$$

$$= \begin{cases} \frac{1}{2\pi} \cos\pi fT \left(\frac{1}{f+1/2T} - \frac{1}{f-1/2T} \right), & |f| \neq 1/2T \\ T/2, & |f| = 1/2T \end{cases} \quad \text{(A-6)}$$

Substitution of (A-6), (2-16) into (A-1) yields

```
q(t) =    cos(Pi/2+Pit/T)/4/Pi [ C1(B(1+E)/2+1/2/T,PiT+2PiT)
                                 -C1(   1/2T       ,PiT+2PiT) ]†
        + cos(Pi/2+Pit/T)/4/Pi [ C1(B(1-E)/2+1/2/T,PiT+2PiT)
                                 -C1(   1/2T       ,PiT+2PiT) ]†
        + sin(Pi/2+Pit/T)/4/Pi [ S1(B(1+E)/2+1/2/T,PiT+2PiT)
                                 -S1(   1/2T       ,PiT+2PiT) ]†
        + sin(Pi/2+Pit/T)/4/Pi [ S1(B(1-E)/2+1/2/T,PiT+2PiT)
                                 -S1(   1/2T       ,PiT+2PiT) ]†
        - cos(Pi/2+Pit/T)/4/Pi [ C1(B(1+E)/2-1/2/T,PiT+2PiT)
                                 -C1(  -1/2T       ,PiT+2PiT) ]†
        - cos(Pi/2+Pit/T)/4/Pi [ C1(B(1-E)/2-1/2/T,PiT+2PiT)
                                 -C1(  -1/2T       ,PiT+2PiT) ]†
        + sin(Pi/2+Pit/T)/4/Pi [ S1(B(1+E)/2-1/2/T,PiT+2PiT)
                                 -S1(  -1/2T       ,PiT+2PiT) ]†
        + sin(Pi/2+Pit/T)/4/Pi [ S1(B(1-E)/2-1/2/T,PiT+2PiT)
                                 -S1(  -1/2T       ,PiT+2PiT) ]†
        + cos(Pi/2-Pit/T)/4/Pi [ C1(B(1+E)/2+1/2/T,PiT-2PiT)
                                 -C1(   1/2T       ,PiT-2PiT) ]†
        + cos(Pi/2-Pit/T)/4/Pi [ C1(B(1-E)/2+1/2/T,PiT-2PiT)
```

```
                          -C1(   1/2T       ,PiT-2PiT) ]†
+ sin(Pi/2-Pit/T)/4/Pi [ S1(B(1+E)/2+1/2/T,PiT-2PiT)
                          -S1(   1/2T       ,PiT-2PiT) ]†
+ sin(Pi/2-Pit/T)/4/Pi [ S1(B(1-E)/2+1/2/T,PiT-2PiT)
                          -S1(   1/2T       ,PiT-2PiT) ]†
- cos(Pi/2-Pit/T)/4/Pi [ C1(B(1+E)/2-1/2/T,PiT-2PiT)
                          -C1(  -1/2T       ,PiT-2PiT) ]†
- cos(Pi/2-Pit/T)/4/Pi [ C1(B(1-E)/2-1/2/T,PiT-2PiT)
                          -C1(  -1/2T       ,PiT-2PiT) ]†
+ sin(Pi/2-Pit/T)/4/Pi [ S1(B(1+E)/2-1/2/T,PiT-2PiT)
                          -S1(  -1/2T       ,PiT-2PiT) ]†
+ sin(Pi/2-Pit/T)/4/Pi [ S1(B(1-E)/2-1/2/T,PiT-2PiT)
                          -S1(  -1/2T       ,PiT-2PiT) ]†
- cos(Pi/2+Pi/2/E/B+Pit/T+Pi/2E) / 8Pi
                [ S1(B(1+E)/2+1/2/T,PiT+Pi/E/B+2Pit)
                  -S1(B(1-E)/2+1/2/T,PiT+Pi/E/B+2Pit) ]
+ sin(Pi/2+Pi/2/E/B+Pit/T+Pi/2E) / 8Pi
                [ C1(B(1+E)/2+1/2/T,PiT+Pi/E/B+2Pit)
                  -C1(B(1-E)/2+1/2/T,PiT+Pi/E/B+2Pit) ]
+ cos(Pi/2+Pi/2/E/B+Pit/T-Pi/2E) / 8Pi
                [ S1(B(1+E)/2-1/2/T,PiT+Pi/E/B+2Pit)
                  -S1(B(1-E)/2-1/2/T,PiT+Pi/E/B+2Pit) ]
+ sin(Pi/2+Pi/2/E/B+Pit/T-Pi/2E) / 8Pi
                [ C1(B(1+E)/2-1/2/T,PiT+Pi/E/B+2Pit)
                  -C1(B(1-E)/2-1/2/T,PiT+Pi/E/B+2Pit) ]
- cos(Pi/2+Pi/2/E/B-Pit/T+Pi/2E) / 8Pi
                [ S1(B(1+E)/2+1/2/T,PiT+Pi/E/B-2Pit)
                  -S1(B(1-E)/2+1/2/T,PiT+Pi/E/B-2Pit) ]
+ sin(Pi/2+Pi/2/E/B-Pit/T+Pi/2E) / 8Pi
                [ C1(B(1+E)/2+1/2/T,PiT+Pi/E/B-2Pit)
```

```
                -C1(B(1-E)/2+1/2/T,PiT+Pi/E/B-2Pit) ]
+ cos(Pi/2+Pi/2/E/B-Pit/T-Pi/2E) / 8Pi
              [ S1(B(1+E)/2-1/2/T,PiT+Pi/E/B-2Pit)
                -S1(B(1-E)/2-1/2/T,PiT+Pi/E/B-2Pit) ]
+ sin(Pi/2+Pi/2/E/B-Pit/T-Pi/2E) / 8Pi
              [ C1(B(1+E)/2-1/2/T,PiT+Pi/E/B-2Pit)
                -C1(B(1-E)/2-1/2/T,PiT+Pi/E/B-2Pit) ]
+ cos(Pi/2-Pi/2/E/B+Pit/T-Pi/2E) / 8Pi
              [ S1(B(1+E)/2+1/2/T,PiT-Pi/E/B+2Pit)
                -S1(B(1-E)/2+1/2/T,PiT-Pi/E/B+2Pit) ]
- sin(Pi/2-Pi/2/E/B+Pit/T-Pi/2E) / 8Pi
              [ C1(B(1+E)/2+1/2/T,PiT-Pi/E/B+2Pit)
                -C1(B(1-E)/2+1/2/T,PiT-Pi/E/B+2Pit) ]
- cos(Pi/2-Pi/2/E/B+Pit/T+Pi/2E) / 8Pi
              [ S1(B(1+E)/2-1/2/T,PiT-Pi/E/B+2Pit)
                -S1(B(1-E)/2-1/2/T,PiT-Pi/E/B+2Pit) ]
- sin(Pi/2-Pi/2/E/B+Pit/T+Pi/2E) / 8Pi
              [ C1(B(1+E)/2-1/2/T,PiT-Pi/E/B+2Pit)
                -C1(B(1-E)/2-1/2/T,PiT-Pi/E/B+2Pit) ]
+ cos(Pi/2-Pi/2/E/B-Pit/T-Pi/2E) / 8Pi
              [ S1(B(1+E)/2+1/2/T,PiT-Pi/E/B-2Pit)
                -S1(B(1-E)/2+1/2/T,PiT-Pi/E/B-2Pit) ]
- sin(Pi/2-Pi/2/E/B-Pit/T-Pi/2E) / 8Pi
              [ C1(B(1+E)/2+1/2/T,PiT-Pi/E/B-2Pit)
                -C1(B(1-E)/2+1/2/T,PiT-Pi/E/B-2Pit) ]
- cos(Pi/2-Pi/2/E/B-Pit/T+Pi/2E) / 8Pi
              [ S1(B(1+E)/2-1/2/T,PiT-Pi/E/B-2Pit)
                -S1(B(1-E)/2-1/2/T,PiT-Pi/E/B-2Pit) ]
- sin(Pi/2-Pi/2/E/B-Pit/T+Pi/2E) / 8Pi
              [ C1(B(1+E)/2-1/2/T,PiT-Pi/E/B-2Pit)
```

-C1(B(1-E)/2-1/2/T,PiT-Pi/E/B-2Pit)]

,E≠0 (A-7)

where S1(x,y)=(A-4), C1(x,y)=(A-5). For $\eta_R=0$ (E=0), only the terms with † are utilized.

APPENDIX B

Derivation of $p(Z,\phi_1)$

The characteristic function of the up-link Gaussian noise $n_1(t)$ in (2-22) is represented by [74]

$$M_{n_{1c}}(u)=\exp[-\sigma_1^2u^2/2] \tag{B-1a}$$

$$M_{n_{1s}}(v)=\exp[-\sigma_1^2v^2/2] \ . \tag{B-1b}$$

Then, the joint p.d.f. $p(n_{1c},n_{1s})$ becomes

$$p(n_{1c},n_{1s}) = \frac{1}{4\pi^2} \int_{-\infty}^{\infty} \exp\{-\sigma_1^2(u^2+v^2)/2\} \cdot \exp\{-(n_{1c}u+n_{1s}v)\}\, du\, dv . \tag{B-2}$$

In Fig.3.1, the up-link composite wave $u_1(t)$ terminates on (Z,ϕ_1). Using (x,y), the point (Z,ϕ_1) is expressed by

$$x = U_0 + I_0\cos\psi_0 + n_{1c} + \sum_{n=1}^{a_1} I_{1n}\cos\psi_{1n} , \tag{B-3a}$$

$$y = I_0 \sin\psi_0 + n_{1s} + \sum_{n=1}^{a_1} I_{1n} \sin\psi_{1n} \cdot \qquad \text{(B-3b)}$$

The joint p.d.f. $p(x,y)$ becomes

$$p(x,y) = \frac{1}{4\pi^2} \int_{-\infty}^{\infty} \int_{-\infty}^{\infty} \exp\{-\sigma_1^2(u^2+v^2)/2\}$$

$$\cdot \prod_{n=1}^{a_1} \exp\{-ju(x/a_1 - U_0/a_1 - I_0\cos\psi_0/a_1 - I_{1n}\cos\psi_{1n})$$

$$-jv(y/a_1 - I_0\sin\psi_0/a_1 - I_{1n}\sin\psi_{1n})\}\, du\, dv \cdot \qquad \text{(B-4)}$$

Representing the point (x,y) with the polar coordinate form as

$$\left.\begin{aligned} x &= Z\cos\phi_1 \\ y &= Z\sin\phi_1 \end{aligned}\right\} \quad (Z \geq 0, \quad 0 \leq \phi_1 \leq 2\pi), \qquad \text{(B-5)}$$

the joint p.d.f. $p(Z,\phi_1)$ becomes

$$p(Z,\phi_1) = \frac{1}{4\pi^2} \int_{-\infty}^{\infty} \int_{-\infty}^{\infty} Z \exp\{-\sigma_1^2(u^2+v^2)/2\}$$

$$\cdot \prod_{n=1}^{a_1} \exp\{-ju(Z\cos\phi_1/a_1 - I_0\cos\psi_0/a_1 - I_{1n}\cos\psi_{1n} - U_0/a_1)$$

$$-jv(Z\sin\phi_1/a_1 - I_0\sin\phi_0/a_1 - I_{1n}\sin\psi_{1n})\}\, du\, dv.$$

$$\qquad \text{(B-6)}$$

Changing the variables as

$$\left.\begin{aligned} u &= \rho\cos\xi \\ v &= \rho\sin\xi \end{aligned}\right\} \quad (\rho \geq 0,\ 0 \leq \xi \leq 2\pi)\ , \tag{B-7}$$

(B-6) becomes

$$p(Z,\phi_1) = \frac{1}{4\pi^2}\int_0^{\infty} d\rho \int_0^{2\pi} d\xi\ Z\rho \exp[-\sigma_1{}^2\rho^2/2 -$$

$$-j\rho\{Z\cos(\xi-\phi_1) - U_0\cos\xi - I_0\cos(\xi-\psi_0)\}]$$

$$\cdot \prod_{n=1}^{a_1} \exp\{j\rho I_{1n}\cos(\xi-\psi_{1n})\}\ . \tag{B-8}$$

Here, the amplitude I_{1n} of the interferer $i_{1n}(t)$ $(n=1,2,\ldots,a_1)$ is constant and the phase ψ_{1n} is uniformly distributed on $(0,2\pi)$. Averaging (B-8) over ψ_{1n}, we get

$$p(Z,\phi_1) = \frac{1}{4\pi^2}\int_0^{\infty} d\rho \int_0^{2\pi} d\xi\ Z\rho \exp[-\sigma_1{}^2\rho^2/2 -$$

$$-j\rho\{Z\cos(\xi-\phi_1) - U_0\cos\xi - I_0\cos(\xi-\psi_0)\}]$$

$$\cdot \prod_{n=1}^{a_1} J_0(I_{1n}\rho)\ , \tag{B-9}$$

where

$$\frac{1}{2\pi}\int_0^{2\pi} \exp[j\rho I_{1n}\cos(\xi-\psi_{1n})]d\psi_{1n} = J_0(\rho I_{1n})\ . \tag{B-10}$$

$J_0(\cdot)$: zero-order first kind Bessel function

Integrating (B-9) over ξ with the relation [70,p.70] :

$$e^{jR\cos\alpha} = \sum_{m=0}^{\infty} \varepsilon_m (-1)^m J_{2m}(R)\cos 2m\alpha + 2j \sum_{m=0}^{\infty} (-1)^m J_{2m+1}(R)\cos(2m+1)\alpha, \tag{B-11}$$

then,

$$p(Z,\phi_1) = \sum_{\nu=0}^{\infty} \frac{\varepsilon_\nu}{2\pi} \cos\nu(\phi_1 - \varepsilon) \int_0^{\infty} Z\rho \exp(-\sigma_1^2\rho^2/2)$$

$$J_\nu(Z\rho)\, J_\nu(V_1\rho) \prod_{n=1}^{a_1} J_0(I_{1n}\rho)\, d\rho \ , \tag{B-12}$$

$$V_1 = [(U_0 + I_0\cos\psi_0)^2 + (I_0\sin\psi_0)^2]^{\frac{1}{2}} \ , \tag{B-13}$$

$$\varepsilon = \tan^{-1}\left[\frac{I_0\sin\psi_0}{U_0 + I_0\cos\psi_0}\right] , \tag{B-14}$$

where ε_m is the Neumann factor and $\varepsilon_0 = 1$, $\varepsilon_m = 2 (m \neq 0)$, and ε is the phase offset due to intersymbol interference as shown in Fig.3.1. Using the relation [70,p.66] :

$$\left(\frac{W}{2}\right)^{-\alpha} J_\alpha(W) = \sum_{\ell=0}^{\infty} \frac{(-1)^\ell \left(\frac{W}{2}\right)^{2\ell}}{\ell!\,\Gamma(\alpha+\ell+1)} \ , \tag{B-15}$$

$p(Z,\phi_1)$ is rewritten as

$$p(Z,\phi_1) = \sum_{\nu=0}^{\infty} \sum_{\eta=0}^{\infty} \sum_{\ell_{11}=0}^{\infty} \cdots \sum_{\ell_{1a_1}=0}^{\infty} \frac{\varepsilon_\nu}{2\pi} \cos\nu(\phi_1 - \varepsilon)$$

$$\frac{(-1)^{\ell_{11}+\ell_{12}+\cdots+\ell_{1a_1}+\eta} V_1^{\nu+2\eta}}{2^{2(\ell_{11}+\ell_{12}+\cdots+\ell_{1a_1}+\eta)+} \eta!\, \Gamma(\nu+\eta+1)}$$

$$\cdot \frac{I_{11}^{2\ell_{11}} \cdots I_{1a_1}^{2\ell_{1a_1}}}{(\ell_{11}!)^2 \cdots (\ell_{1a_1}!)^2} \int_0^{\infty} Z\rho^{2(\ell_{11}+\ell_{12}+\cdots+\ell_{1a_1}+\eta)+\nu+1}$$

$$\cdot \exp[-\sigma_1^2\rho^2/2] J_\nu(Z\rho)\, d\rho \ , \qquad \text{(B-16)}$$

where $\Gamma(\cdot)$ is the Gamma function.

Using the Bessel integral relationship [77,p.393]

$$\int_0^{\infty} J_\nu(at) \exp(-p^2 t^2) t^{\mu-1} dt = \frac{\Gamma(\frac{\nu}{2}+\frac{\mu}{2})(\frac{a}{2p})^\nu}{2p^\mu\, \Gamma(\nu+1)}$$

$$\cdot {}_1F_1[\tfrac{\nu}{2}+\tfrac{\mu}{2} ; \nu+1; -\tfrac{a^2}{4p^2}]$$

$$\mathrm{Re}(\mu+\nu)>0, \quad |\mathrm{Arg}p| < \frac{\pi}{4} \qquad \text{(B-17)}$$

in (B-16) for integration over Z, the desired p.d.f. $p(Z,\phi_1)$ is obtained in (3-1).

APPENDIX C

The Gram-Charlier Expansion

We express the unknown p.d.f. $p(x)$ whose moments are known using succesive derivatives of the normal function as [79],[80]

$$p(x) = \sum_{p=0}^{\infty} \hat{F}(p)\ y^{(p)}(x)\ , \tag{C-1}$$

where

$$y^{(p)}(x) = \frac{d^p}{dx^p}\ \frac{1}{\sqrt{2\pi}}\ \exp(-x^2/2)$$

$$= \frac{(-1)^p}{\sqrt{2\pi}} \exp(-x^2/2)\ H_p(x)\ . \tag{C-2}$$

After multiplying both sides of (C-1) by $H_q(x)$, we integrate the result term by term between $(-\infty, \infty)$.

$$\int_{-\infty}^{\infty} p(x)\ H_q(x)\ dx = \sum_{p=0}^{\infty} \frac{\hat{F}(p)}{\sqrt{2\pi}}\ (-1)^p \int_{-\infty}^{\infty} H_p(x)\ H_q(x)\ \exp(-x^2/2)\ dx \tag{C-3}$$

Now using the orthogonality of Hermite polynomials

$$\int_{-\infty}^{\infty} H_p(x)\ H_q(x)\ \exp(-x^2/2)\ dx = \begin{cases} \sqrt{2\pi}\ p! \\ 0\ , \quad p \neq q \end{cases}\ , \tag{C-4}$$

then the coefficient $\widehat{F}(p)$ in (C-1) is obtained as

$$\widehat{F}(p)=\frac{(-1)^p}{p!}\ F(p)\ , \tag{C-5}$$

$$F(p) = \int_{-\infty}^{\infty} p(x)\ H_p(x)\ dx\ . \tag{C-6}$$

Expanding $H_p(x)$, $F(p)$ is rewritten with the moments of $p(x)$ to get (4-21). Therefore the desired series expansion of $p(x)$ is represented by (4-20) and (4-21).

REFERENCES

[1] S. Stein and J. J. Jones, Modern Communication Principles. New York : McGraw-Hill, 1967.

[2] H. Taub and D.S. Schilling, Principles of Comminication Systems, New York : McGraw-Hill, 1960.

[3] A. B. Carlson, Communication Systems, second edition, New York : McGraw-Hill, 1975.

[4] M. Schwarz, Information Transmission, Modulation and Noise. Tokyo : McGraw-Hill Kogakusha,Ltd., 1959.

[5] H.C. van den Elten and P.van der Wurf : " A Simple Method of Calculating the Characteristics of FSK Signal with Modulation Index 0.5, " IEEE Trans. Commun., Vol.COM-20, No.2, pp. 139-147, April 1972.

[6] J. Fuenzalida, P. Rivalan and H.J. Weiss : " Summary of the INTELSAT V Communication Performance Specifications," COMSAT Tech. Rev., Vol.7, No.1, pp.311-326, Spring 1977.

[7] H. Yokoi and T. Muratani : " Satellite Communications in the INTELSAT V Era," The Journal of IECE of Japan, Vol.61, No.9, pp.992-998, September 1978 (in Japanese).

[8] J.J. Spilker,Jr., Digital Communications by Satellite. New Jersey : Prentice-Hall, 1977.

[9] V.K. Bhargava, D. Haccoun, R. Matyas, and P. Nuspl, Digital Communications by Satellite. New York : John Wiley and Sons, 1981.

[10] G. Satoh and T. Mizuno :" Nonlinear Satellite Channel Design for QPSK/TDMA Transmission, " Fifth International Conference of Digital Satellite Communications, Section II.A, pp.47-54,

March 1981.

[11] N. Morinaga and I. Oka : " Research Toward Digital Communi- Over the Nonlinear Channels," The Journal of IECE of Japan, Vol.65, No.9, pp.1007-1009, September 1982 (in Japanese).

[12] A. S. Rosenbaum :" PSK Error Performance with Gaussian Noise and Interference, " Bell Syst. Tech. J., Vol.48, pp.413-442, February 1969.

[13] V.K. Prabhu :" Error Rate Considerations for Coherent Phase-Shift Keyed Systems with Co-Channel Interference,"Bell Syst. Tech. J., Vol.48, pp.743-767, March 1969.

[14] J. Goldman :" Multiple Error Performance of PSK Systems with Cochannel Interference and Noise, " IEEE Trans. Commun.,Vol. COM-19, No.4, pp.420-430, August 1971.

[15] J.J. Jones :" Filter Distortion and Intersymbol Interference Effects on PSK Signals, " IEEE Trans. Commun., Vol. COM-19, No. 2, pp.120-132, April 1971.

[16] V. K. Prabhu : " Performance of Coherent Phase-Shift-Keyed Systems with Intersymbol Interference,"IEEE Trans.Inf.Theory, Vol.IT-17, pp.418-431, July 1971.

[17] B. R. Saltzberg : " Intersymbol Interference Error Bounds with Application to Ideal Bandlimited Signaling,"IEEE Trans. Inf. Theory, Vol. IT-14, No.4, pp.563-568, July 1968.

[18] R. Lugannani : " Intersymbol Interference and Probability of Error in Digital Systems, " IEEE Trans. Inf. Theory, Vol. IT-15, No.6, pp.682-688, November 1969.

[19] O.Shimbo and M.I. Celebiler : " The probability of error due to Intersymbol interference and Gaussian noise in Digital Communication Systems, " IEEE Trans. Commun., Vol. COM-19, No.2, pp.113-119, April 1971.

[20] O. Shimbo, R. J. Fang, and M.I. Celebiler :" Performance of

M-ary PSK Systems in Gaussian Noise and Intersymbol interference, " IEEE Trans. Inf. Theory, Vol.IT-19, No.1, pp.44-58, January 1973.

[21] S.Benedetto, E.Biglieri, and V.Castellani," Combined Effects of Intersymbol Interference and Co-Channel Interferences in M-ary CPSK Systems, " IEEE Trans. Commun., Vol.COM-21,No.10, pp.997-1008, September 1973.

[22] M. I. Celebiler and G. M. Coupe : " Probability of Error for Coherent PSK in the Presence of Thermal Noise and Intersymbol, Interchannel, and Co-Channel Interferences," IEE Conf. Publ. (GBR), No.126, pp.146-155, 1975.

[23] R. J. Fang and O. Shimbo : " Unified Analysis of a Class of Digital Systems in Additive Noise and Interference, " IEEE Trans.Commun., Vol.COM-21,No.10, pp.1075-1082, October 1973.

[24] S. Benedetto, G. Vincentiis, and A. Luvison : " Error Probability in the Presence of Intersymbol Interference and Additive Noise for Multilevel Digital Signal,"IEEE Trans.Commun., Vol. COM-21, No. 3, pp.181-190, March 1973.

[25] V. K. Prabhu : " MSK and Offset QPSK Modulations with Band-limiting Filters, " IEEE Trans. Aerosp. and Electron. Syst., Vol. AES-17, No.1, pp.2-8, January 1981.

[26] J.R. Cruz and R.S. Simon: " Cochannel and Intersymbol Intersymbol Interference in Quadrature-Carrier Modulation Systems, " IEEE Trans. Commun., Vol. COM-29, No.3, pp. 285-297, March 1981.

[27] V.K.Prabhu :" PSK-Type Modulation with Overlapping Base Band Pulses, " IEEE Trans. Commun., Vol.COM-25, No.9, pp.980-990, September 1970.

[28] F.Assal, K.Betaharon, and C.Mahle : " 4 Phase PSK-PCM Transmission Through Linear and Non-Linear Channels," Technical

Memorandom of COMSAT Laboratory, No.CL51-76, Octobeer 1976.

[29] P. C. Jain : " Modulation / Coding for Bandlimited Nonlinear Satellite Channels, " Text for the tutorial by NTC and IEEE Communication Society, Los Angels, December 1977.

[30] C. Devieux,Jr :" QPSK Bit-Error Rate Performance as affected by Cascaded linear and Nonlinear elements,"COMSAT Tech.Rev., Vol. 8, No. 1, pp.205-218, Spring 1978.

[31] J.C.Y. Huang and K. Feher :" Performance of QPSK, OKQPSK and MSK Signals through a Satellite Link,"IEEE 1978 Canadian Communication and Power Conf., pp.86-89, 1978.

[32] S. Murakami, Y. Furuya, Y. Matsuo, and M. Sugiyama :"Optimum Modulation and Channel Filters for Nonlinear Satellite Channels," IEEE Trans. Commun., Vol.COM-27, No.12, pp.1810-1819, December 1979.

[33] R.J. Fang :" Quaternary Transmission Over Satellite Channels with Cascaded Nonlinear Elements and Adjacent Channel Interference," IEEE Trans. Commun., Vol.COM-29, No.5, pp.567-581, May 1981.

[34] C.Devieux,Jr. :" A Practical Optimization Approach for QPSK/ TDMA Satellite Channel Filtering, " IEEE Trans.Commun., Vol. COM-29, No. 5, pp.556-566, May 1981.

[35] Y. Yoshida and T.Hatsuda : " Transmission Characteristics in PCM-PSK Satellite Systems," Memorandom of Electrical Communication Raboratory of NTT, march 1977 (in Japanese).

[36] M. R. Wachs and D. E. Weinreich :" A Laboratory Study of the Effects of CW Interference on Digital Transmission over Nonlinear Channels, " Third International Conference on Digital Satellite Communications, No.B-3, pp.65-72, November 1975.

[37] T. Muratani, H. Saito, K. Koga, and Y. Yasuda :" Final Study Report for IS-838 High Speed Forward Error Correction Codec,"

KDD Technical Note, No.138, January 1978.

[38] C. R. Cahn : " A Note on Signal-to-Noise Ratio in Bandpass Limiters," IRE Trans. Inf. Theory, Vol.IT-7, No.1, pp.39-43, January 1961.

[39] J.M. Aein and W. Doyle : "A Note on Cascaded Limiters," IEEE Trans. Space Electronics and Telemetry, Vol.SET-11,pp.47-49, March 1965.

[40] S. M. Arastoo, N. Morinaga, T. Namekawa : " SNR Performances for Cascaded Hard Limiting Repeater System, " IEEE Trans. Cable Television, Vol.CATV-3, No.2, pp.49-57, April 1978.

[41] W. B. Davenport and W. L. Root, Random Signal and Noise. New York : McGraw-Hill,1960.

[42] D. Middleton, An Introduction to Statistical Communication Theory. New York : McGraw-Hill, 1960.

[43] J.J. Jones : "Hard-Limiting of Two Signals in Random Noise," IEEE Trans.Inf.Theory, Vol.IT-9,No.1,pp.34-42, January 1963.

[44] N. M. Blackman : " The Signal X Signal, Noise X Noise, and Signal X Noise Output of a Nonlinearity, " IEEE Trans, Inf. Theory, Vol.IT-14, No.1, pp.21-27, January 1968.

[45] J. C. Springett and M. K. Simon : " An Analysis of the Phase Coherent - Incoherent Output of the Bandpass Hard Limiter," IEEE Trans. Commun., COM-19, No.1, pp.42-49, February 1971.

[46] P. C. Jain and N. M. Blackman : " Detection of a PSK Signal Transmission Through a Hard-Limited Channel, " IEEE Trans. Inf. Theory, Vol.IT-19, No.5, pp.623-630, September 1973.

[47] A. W. Weinberg :" Effects of a Hard Limiting Repeater on the Performance of a DPSK Data Transmission System," IEEE Trans. Commun., Vol.COM-25, No.10, pp.1128-1133, October 1977.

[48] J.S.Lee, R.H. French, and Y.K. Hong : " Error Performance of Binary DPSK Data Transmission on the Hard-Limiting Satellite

Channel," IEEE Trans.Inf.Theory, Vol.IT-4, No.4, pp.489-497, July 1981.

[49] T.Mizuno, N.Morinaga and T.Namekawa :" Transmission Characteristics of an M-ary Coherent PSK Signal Via a Cascade of N Bandpass Hard Limiters,"IEEE Trans.Commun.,Vol.COM-24, No. 5, pp.540-545, May 1976.

[50] W. C. Lindsey, Telecommunication System Engineering. Englewood Criffs, New Jersey : Prentice-Hall, 1973.

[51] N. Ekanayake and D. P. Taylor : " CPSK Signaling over Hard Limited Channels in Additive Gaussian Noise and Intersymbol Interference," IEEE Trans. Inf. Theory, Vol.IT-25, No.1, pp. 62-68, January 1979.

[52] N. Ekanayake and D. P. Taylor : " Binary CPSK Performance Analysis for Saturating Band-Limited Channels," IEEE Trans., Commun., Vol.COM-27, No.3, pp.596-603, March 1979.

[53] R. G. Lyons : " The Effects of a Bandpass Nonlinearity on Signal Detectability,"IEEE Trans. Commun., Vol.COM-21, No.1, pp.51-60, January 1973.

[54] N. M. Blackman : " The Output Signals and Noise from a Nonlinearity with Amplitude Dependent Phase Shift," IEEE Trans. Inf. Theory, Vol.IT-25, No.1, pp.77-79, January 1979.

[55] D.J. Kenedy and O. Shimbo : " Cochannel Interference in Nonlinear QPSK Satellite Systems, " IEEE Trans. Commun., Vol. COM-29, No.5, pp.582-592, May 1981.

[56] P.Hetrakul and D.P. Taylor :"The Effects of Satellite Transponder Nonlinearities on the Performance of Binary PSK Systems, " Third International Conference on Digital Satellite Communications, No.B-3, pp.49-55, November 1975.

[57] M. Dahabreh, N. Morinaga, and T. Namekawa : " An Analysis of Output Characteristics of Nonlinear Satellite Transponder

for Multi-Carrier Systems, " IECE of Japan Trans., Vol. E64, No.5, pp.334-341, May 1981.

[58] S. Benedetto, E. Biglieri, and R. Daffara : " Modeling and Performance Evaluation of Nonlinear Satellite Links - A Volterra Series Approach," IEEE Trans. Aerosp. and Electron. Syst., Vol.AES-15, No.4, pp.494-507, July 1979.

[59] E.Bedrosian and S.O.Rice :"The Output Properties of Volterra Systems (Nonlinear Systems with Memory) Driven by Harmonic and Gaussian Inputs, " IEEE Proc., Vol. 59, No.12, pp.1688-1707, December 1971.

[60] M. Rudko and D. Weiner:"Volterra Systems with Random Inputs: A formalized Approach," IEEE Tran.Commun., Vol.COM-26, No.2, pp.217-227, February 1978.

[61] M. Schetzen, The Volterra and Wiener Theory of Nonlinear Systems. New York : John Wiely and Sons, 1980.

[62] C. M. Chie : " A Modified Barett-Lamperd Expansion and Its Application to Bandpass Nonlinearities with Both AM-AM and AM-PM Conversion, " IEEE Trans. Commun., Vol. COM-28, No.11, pp.1859-1866, November 1980.

[63] T.C. Huang, J.K. Omura, and W.C. Lindsey : " Analysis of Coherent Satellite Communication Systems in the Presence of Interference and Noise," IEEE Trans. Commun., Vol.COM-29,No. 5, pp. 593-604, May 1981.

[64] S. O. Rice : Mathematical Analysis of Random Noise," Bell Syst. Tech. J., Vol.23, pp.282-332,1944 ; and Vol.24, pp.46-156, 1945.

[65] I.Oka, S.Kabasawa, N.Morinaga, and T.Namekawa : " PSK Signal Transmission Characteristics through Nonlinear Satellite Repeater with Cochannel Interferences Part 1," IECE of Japan Technical Group on Communication System, Vol.CS78-13,pp.1-8,

May 1978 (in Japanese).

[66] I.Oka, S.Kabasawa, N.Morinaga, and T.Namekawa : " PSK Signal Transmission Characteristics through Cascaded Nonlinear Repeaters in Electro - magnetic Interferences Environment," IECE of Japan, 1989 National Conference Records, No.1785, p. 7-224, March 1979 (in Japanese).

[67] I.Oka, S.Kabasawa, N.Morinaga, and T.Namekawa : " PSK Signal Transmission Characteristics through N-Cascaded Nonlinear Repeater with Electro-magnetic Interferences Part II ," IECE of Japan Technical Group on Electromagnetic Compatibility, Vol.EMCJ 78-60, pp.29-34, Januarly 1979 (in Japanese).

[68] I.Oka, S.Kabasawa, N.Morinaga, and T.Namekawa:" Transmission Characteristics of PSK Signal through Cascaded Bandpass Hard Limiters with Interferences, "IECE of Japan Trans.,Vol.63-B, pp.203-210, March 1980 (in Japanese).

[69] I.Oka, S.Kabasawa, N.Morinaga, and T.Namekawa:" Interference Immunity Effects in CPSK Systems with Hard-Limiting Transponders," IEEE Trans. Aerosp. and Electron. Syst., Vol. AES-17, No.1, pp.93-100, January 1981.

[70] W. Magnus, F. Oberhettinger, and R.P. Soni, Formula Theorems for the Special Functions of Mathematical Physics. New York : Springer-Verlag, 1966.

[71] J.M. Wozencraft and I.M. Jacobs, Principles of Communication Engineering. New York : John Wiley and Sons, 1967.

[72] I.Oka, N.Morinaga, and T.Namekawa:" Effects of Soft-Limiting in PSK Satellite Systems, " To be published by Archiv fuer Elektronik und Uebertragungstechnik.

[73] I.Oka, N.Morinaga, and T.Namekawa : " Improvements of Binary PSK Signal Transmission Characteristics via Soft-Limiter in Interference Environments, " Proceeding of the 4th Symposium

on Information and Its Application, pp.489-494, December 1981 (in Japanese).

[74] A. Papoulis, Probability, Random Variables and Stochastic Process. New York : McGraw-Hill, 1965.

[75] I.Oka, N.Morinaga, and T.Namekawa:" Modeling and Analysis of MSK Signal Transmission via Bandpass Hard Limiter," IECE of Japan,1982 National Conference Records, No.1761, p.7-203, March 1982 (in Japanese).

[76] I.Oka, N.Morinaga, and T.Namekawa : " Transmission Characteristics QPSK, OQPSK, and MSK in Hard-Limited Interfering Channels,"IECE of Japan, Records of 1982 National Conference on Communication Engineering, No. 548, p.7-284 , August 1982 (in Japanese).

[77] G. N. Watson, A Treates on the Theory of Bessel Functions. New York : Cambridge Univ. Press, 1922.

[78] I. S. Gradshteyn and I.M. Ryzhik, Table of Integrals, Series and Products. New York : Achademic Press, 1980.

[79] M. G. Kendall, The Advanced Theory of Statistics. London: Charles Griffin and Company Limited, 1943.

[80] T. C. Fry, Probability and Its Engineering Uses. New York : D.Van Nostrand Co., 1965.